

AD



Research and Development Technical Report
ECOM-3281

AD708542

SPECTRAL EMITTANCE OF
NEODYMIUM, SAMARIUM, ERBIUM AND
YTTERBIUM OXIDES AT HIGH TEMPERATURE

by

Guido E. Guazzoni
Stuart J. Shapiro

May 1970

DISTRIBUTION STATEMENT (1)

This document has been approved for public
release and sale; its distribution is unlimited.

E**C****O****M**

UNITED STATES ARMY ELECTRONICS COMMAND • FORT MONMOUTH, N.J.

45

NOTICES

Disclaimers

The findings in this report are not to be construed as an official Department of the Army position, unless so designated by other authorized documents.

The citation of trade names and names of manufacturers in this report is not to be construed as official Government endorsement or approval of commercial products or services referenced herein.

Disposition

Destroy this report when it is no longer needed. Do not return it to the originator.

Reports Control Symbol OSD-1366

TECHNICAL REPORT ECOM-3281

SPECTRAL EMITTANCE OF
NEODYMIUM, SAMARIUM, ERBIUM AND YTTERBIUM OXIDES AT HIGH TEMPERATURE

Guido E. Guazzoni and Stuart J. Shapiro
Power Sources Division
Electronic Components Laboratory

MAY 1970

LTO 61102 A 34 A 02

Distribution Statement (1)

This document has been approved
for public release and sale;
its distribution is unlimited.

US ARMY ELECTRONICS COMMAND
FORT MONMOUTH, NEW JERSEY

ABSTRACT

Spectral emittance of solid specimens of Er_2O_3 , Yb_2O_3 , Sm_2O_3 and Nd_2O_3 has been obtained by comparison of sample emission with the emission of a standard black body cavity maintained at the same sample true temperature. The spectral emittance has been characterized in a wavelength range of 0.4 - 5.0 micrometer and at sample temperatures from 1520°K up to 1870°K corresponding to surface radiation flux densities of 10 - 50 W/cm^2 . This flux density range is of practical interest for thermo-photovoltaic energy conversion applications. Preliminary observations of spectral transmittance and reflectance are also reported.

CONTENTS

	<u>Page</u>
INTRODUCTION	1
DISCUSSION	1
Sample Preparation	1
Flame Emission	2
Sample Transmittance	2
Sample Emittance	4
1. Thermocouple Method	8
2. Cavity Method	12
3. Spectral Emittance	14
Sample Absorptance and Reflectance	20
CONCLUSIONS	29
REFERENCES	30

FIGURES

1. Cross Section of an $\text{Er}_2\text{O}_3 / \text{Yb}_2\text{O}_3$ Specimen Utilized in Transmittance Test	3
2. Sample Oxy-Propane Torch Assemblage for Transmittance Test	4
3. Comparison of the Radiation from Real Body and Black Body	6
4. Location of the Thermocouple Junction Inside the Specimen	8
5. Er_2O_3 and Yb_2O_3 Specimens with Thermocouple Implanted	9
6. Two-Torch Apparatus Used for Maintaining the Same Brightness Temperature on Both Sides of the Specimen	10
7. Location of the Two Parallel Platinum Electrodes Inside the Specimen	11
8. Section of Yb_2O_3 and Er_2O_3 Specimens Showing the Location of Cylindrical Cavities	12
9. Cross Section of the Cylindrical Cavities Formed into the Specimens Used	13

CONTENTS

Page

FIGURES (CONT)

10. Emittance of Nd_2O_3 , Er_2O_3 , Sm_2O_3 and Yb_2O_3 in a Temperature Range Between 1500 and 2000° K	15
11. Schematic of the Instrumentation Assembly Utilized for the Emittance Spectra	16
12. Instrumentation Assembly	17
13. Spectral Emittance of Er_2O_3 in a Wavelength Range from .45 μm to 1.9 μm	21
14. Spectral Emittance of Er_2O_3 in a Wavelength Range from 1.8 μm to 4.8 μm	22
15. Spectral Emittance of Sm_2O_3 in a Wavelength Range from 0.6 μm to 2.1 μm	23
16. Spectral Emittance of Sm_2O_3 in a Wavelength Range from 2.0 μm to 5.0 μm	24
17. Spectral Emittance of Nd_2O_3 in a Wavelength Range from 0.55 μm to 2.0 μm	25
18. Spectral Emittance of Nd_2O_3 in a Wavelength Range from 1.8 μm to 4.8 μm	26
19. Spectral Emittance of Yb_2O_3 in a Wavelength Range from 0.4 μm to 1.9 μm	27
20. Spectral Emittance of Yb_2O_3 in a Wavelength Range from 1.8 μm to 4.8 μm	28
21. Er_2O_3 Electrical Resistance Characteristics	33
22. Relative Eye Luminosity Factor and Optical Transmittance of the Corning #2403 Red Glass Filter	35
23. Pyrometer Filter Band-Pass Characteristic	36
24. Effective Wavelength for any Temperature Interval in the Range 1300 to 3000° K	37

APPENDIXES

A. Evaluation of Sample Resistivity	32
B. Determination of Pyrometer Effective Wavelength	34

SPECTRAL EMITTANCE OF
NEODYMIUM, SAMARIUM, ERBIUM AND YTTERBIUM OXIDES AT HIGH TEMPERATURE

INTRODUCTION

Preliminary spectral analysis of a group of rare earth oxides established the potential of these materials as selectively radiating thermal sources for thermophotovoltaic energy conversion^{1,2} and allowed a selection of the most appropriate of these oxide emitters for spectral matching with the response characteristic of germanium and silicon photovoltaic cells for optimum conversion efficiency.³

Spectral normal emittance data for rare earth oxides over a broad spectral range and at temperatures up to 1800° K are generally unavailable. Recent work at these refractory temperatures reported emittances only in the visible region of the spectrum and not in sufficient detail to be fully useful for thermophotovoltaic conversion analysis.^{4,5} To provide additional basic spectral emittance data on this interesting class of materials, a more detailed program was planned covering the spectrum range of 0.45 μm to 5.0 μm over the temperature regime of 1540° K to 1870° K. The present study will consider the rare earth oxides of Erbium, Ytterbium, Samarium and Neodymium. In addition, preliminary indications of spectral transmittance and reflectance are reported.

DISCUSSION

Sample Preparation

With the concept in mind that the term "emissivity" is reserved for pure (idealized) specimens,⁶ the term "emittance" has been used here as characteristic of the particular samples prepared for this study. The samples of Er_2O_3 , Yb_2O_3 , Sm_2O_3 and Nd_2O_3 were prepared from 99.9 percent pure oxide powder having a mean particle size < 5 μm . These were die formed in the shape of one-inch-diameter discs and pressed at pressures from 10,000 to 20,000 psi to obtain wafers of approximately equal apparent density of 4.5. The thickness of the specimens was approximately 1 mm with the exception of the specimens utilized in the tests described in Paragraph 2 (Cavity Method). The materials and the preparation procedure were the same as those previously reported.^{2,3}

Samples were mounted in a refractory material holder and heated with an oxygen-propane torch to temperatures ranging from 1520° K up to 1870° K, corresponding to surface radiation flux densities of 10-50 watts/ cm^2 which is the range of practical interest for thermophotovoltaic energy conversion applications.

Flame Emission

The use of oxygen-propane flames to thermally excite the rare earth oxide samples imposed an investigation of the flame emission in the entire spectral range of interest. For this purpose the free flame was located at the same normal specimen position, and its emission spectrophotometrically sampled from $0.4 \mu\text{m}$ to $5.0 \mu\text{m}$, for the same solid angle as was used to record the rare earth oxide spectra.

For wavelengths between $0.4 \mu\text{m}$ and $1.3 \mu\text{m}$, the free flame emission did not exceed values greater than 1.7×10^{-3} of the corresponding spectral emission of the solid specimens at the lowest investigated temperature. Pyrometric measurements indicated apparent flame brightness temperatures around 1050°K . This temperature corresponds to the amount of radiant energy as seen by the pyrometer at $\lambda = 0.66 \mu\text{m}$ (pyrometric working wavelength) which is about 1.5×10^{-3} times the corresponding radiant energy sampled, by the same instrument, from the rare earth oxide specimens. This is in agreement with the emission ratio spectrophotometrically recorded.

Between 1.3 and $2.4 \mu\text{m}$ the flame shows two broad emission bands. The first, which is centered around $1.5 \mu\text{m}$, in the same wavelength region where the Er_2O_3 has its strong emission peak, does not exceed 6×10^{-3} times the corresponding Er_2O_3 emission. The second, around $1.9 \mu\text{m}$, reaches values as high as 1.5×10^{-2} times the corresponding spectral emission of the Er_2O_3 which has the lowest emission, in this wavelength region, of the four rare earth oxides tested.

Beyond $2.4 \mu\text{m}$ the emission spectrum of the oxy-propane flame shows two other bands reaching absolute (black body referenced) emission values more competitive with the corresponding emission of Yb_2O_3 and Er_2O_3 which, of the oxides tested, gave the lowest emission in this infrared region. The band ranging from $2.4 \mu\text{m}$ to $3.0 \mu\text{m}$ reaches, at $2.85 \mu\text{m}$, a relative value as high as 10^{-1} of the corresponding Yb_2O_3 emission. From $3 \mu\text{m}$ to $4.15 \mu\text{m}$ the flame emission does not exceed 2×10^{-2} times the corresponding rare earth oxides values, but at $4.2 \mu\text{m}$ a second broad band appears extending out to $4.5 \mu\text{m}$ with values as high as 50% the corresponding samples emission.

From these observations, the following conclusions were drawn:
(1) Flame emission up to $2.4 \mu\text{m}$ is not significant enough to invalidate the method of emittance measurements. (2) With the flame source positioned behind the heated sample there is no enhancement of the specimen emission due to the flame emission, provided the samples are not transparent beyond $2.4 \mu\text{m}$. (3) When an additional flame source is used in front of the sample, only emission data beyond $2.4 \mu\text{m}$ require minor correction to account for the flame bands at 2.85 and $4.3 \mu\text{m}$.

Sample Transmittance

To properly evaluate the sample emittance in spectral regions where the flame source has emission bands, it is necessary to demonstrate that the specimens are not significantly transparent. For this purpose the

emission spectra were recorded for samples which consisted of composites of two different rare earth oxides. These specimens, in the shape of one-inch-diameter wafers, were die formed pressing together two wafers of different rare earth oxide powders, about 0.5 mm thick, in order to obtain specimens 1 mm total thickness. Figure 1 shows a cross section of a composite specimen.

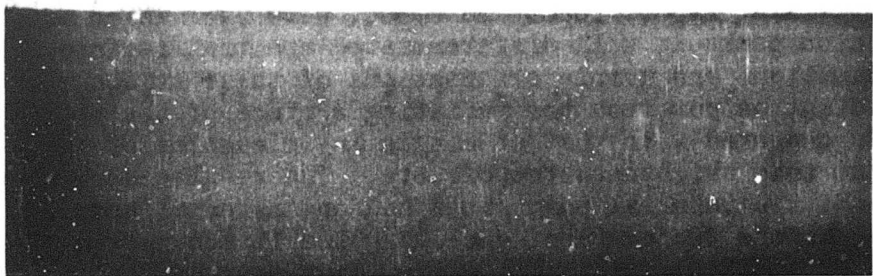


Fig. 1 - Cross Section of an Er_2O_3 / Yb_2O_3 Specimen Utilized in Transmittance Test

For this experiment the arrangement of flame source and pellet sample was as shown in Figure 2. The flame, impinging on the pellet, directly heats the first layer. The second layer of the composite is heated, by conduction, to the test temperature and emission from its outer surface is sampled spectrophotometrically.

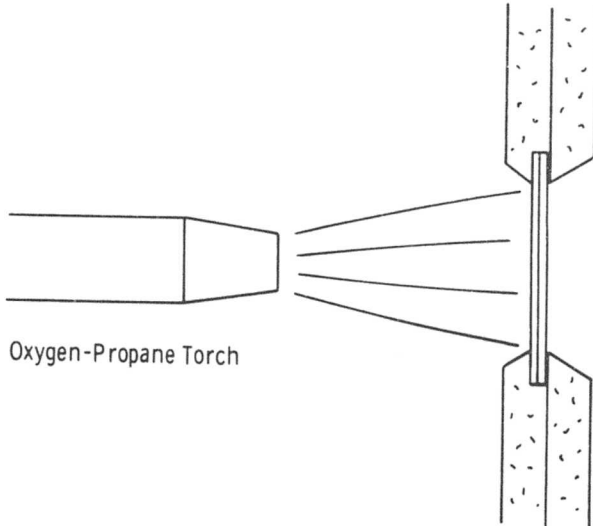


Fig. 2 - Sample Oxy-Propane Torch Assemblage for Transmittance Test

Three materials, Er_2O_3 , Yb_2O_3 and Sm_2O_3 , were used which show characteristic emission peaks in well differentiated spectral regions. All possible combinations and sample orientations of these oxides were evaluated. The radiant output from the radiating surface of the two layer composites was compared with that of single layer samples of the same material at the same brightness temperature. The results showed no variation between the two material composites and one material samples, at the same emitting surface temperature, exceeding the 1% accuracy of the recording instrumentation used. Therefore, over the range of $1570\text{-}1970^\circ \text{K}$, it is concluded that 0.5 mm specimens of these materials can be considered opaque between 0.4 and $5.0 \mu\text{m}$. This also means that experimental evidence has been obtained that rare earth oxide emitters for thermophotovoltaic converters may be prepared using any mechanically and chemically compatible refractory substrate without regard for its spectral emission.

Sample Emittance

The procedure devised to obtain spectral emittance characteristics of the rare earth oxide specimens was based on the knowledge of the emittance value of these materials for at least one wavelength and on the simultaneous spectrophotometric sampling of the emission spectra from the specimen and from a high temperature black body reference source, each maintained at the same true temperature.

In the absence of valid emittance data from the basic literature concerning these oxides in the high temperature regime of interest, the first part of this experimental investigation was concentrated on obtaining

emittance values of our specimens at the wavelength of $0.66 \mu\text{m}$ in a temperature interval from 1470°K to 1870°K . Two alternative methods were selected for the evaluation of the emittance at $\lambda = 0.66 \mu\text{m}$. Both are based on measurements of true temperature and brightness temperature of the samples.

In connection with the use of an optical pyrometer for the surface brightness temperature measurement, the first method utilizes the output of a thermocouple implanted into the specimen for the evaluation of its true temperature. The second method is based on direct optical pyrometric readings of both surface brightness temperature and true sample temperature. The true sample temperature was obtained by sampling the radiation from small cylindrical cavities, drilled into the specimens, which acted as black body radiator cavities.

For a better understanding of the correlation between pyrometric measurements and the spectrophotometric procedure devised, it is useful to review some of the basic concepts of optical pyrometry.⁷ If the radiating samples to be investigated are opaque solids, their radiation can be described by the following modified form of Planck's radiation equation for the spectral distribution of radiant energy as a function of the temperature;

$$dE = \epsilon(\lambda) A J(\lambda, T) d\lambda = \epsilon(\lambda) A c_1 \frac{d\lambda}{\lambda^5 \left[e^{\frac{c_2}{\lambda T}} - 1 \right]} \quad (1)$$

where: dE = emitted radiant energy per unit time (watts) for a differential wavelength interval $d\lambda$

$\epsilon(\lambda)$ = spectral emittance

A = area from which emission takes place (square cm)

$J(\lambda, T)$ = energy emitted per unit time per unit area per unit wavelength interval uniformly over a solid angle of 2π steradians

λ = wavelength (microns)

T = absolute temperature ($^\circ \text{K}$)

$c_1 = 3.7413 \times 10^{-4} \text{ watts/cm}^2 \cdot \text{sr} \cdot \mu\text{m}^2$

$c_2 = 1.4388 \times 10^{-4} \mu\text{m} \cdot \text{sr} \cdot \text{K}$

Although $J(\lambda, T)$ describes black body radiation only, $\epsilon(\lambda)$ is so defined that $\epsilon(\lambda) J(\lambda, T)$ describes the radiation from a real body. Under the same geometric conditions, and at the same wavelength λ , the ratio of real body radiation to black body radiation, when both sources are at the same absolute temperature, is called spectral emittance;

$$\epsilon(\lambda) = \frac{J(\lambda, T) \text{ from real body}}{J(\lambda, T) \text{ from black body}} \quad (2)$$

Consider a real body at a true temperature T (Fig. 3). Its spectral distribution of radiant energy will be, at any wavelength, less than the corresponding radiation from a black body radiator at the same true temperature T .

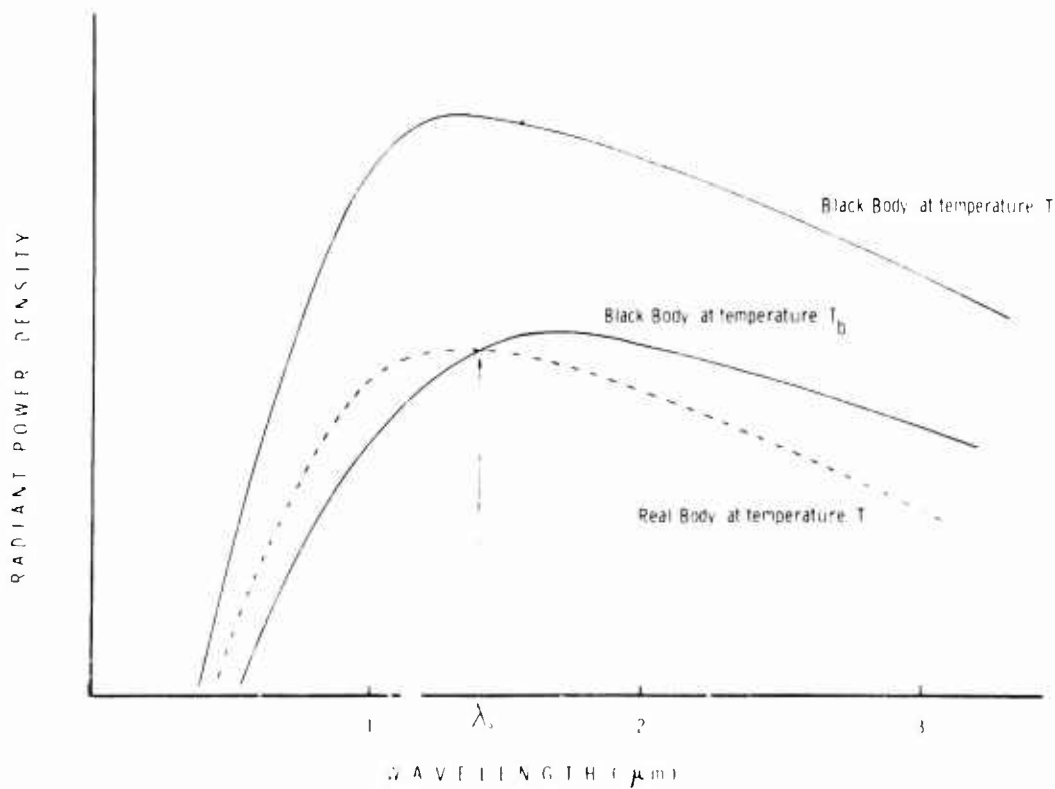


Fig. 3 - Comparison of the Radiation from Real Body and Black Body

At any particular wavelength λ_0 , however, there is a black body temperature T_b , less than T , such that the real body radiation in a differential wavelength interval around λ_0 is equal to the black body radiation at temperature T_b , in the same spectral interval. The temperature T_b is then called the monochromatic brightness temperature of the real body at wavelength λ_0 .

For any real body at true temperature T , the brightness temperature T_b may vary with wavelength in accordance with variation in emittance with wavelength. When using brightness temperature it is necessary to specify the wavelength with which the brightness temperature is associated. To estimate the temperature of a real body one can measure $J(\lambda, T)$ relative to some standard spectral radiance, and then define a temperature scale based on the ratio of two spectral radiances, one of which is selected as a standard. A brightness temperature pyrometer is a device that translates the measurement of $J(\lambda, T)$ into a brightness temperature scale. Sampling the energy radiated by the real body described in Fig. 3, the temperature it will indicate is T_b , because it cannot distinguish between the real body whose temperature is T and a black body whose temperature is T_b , when operated at wavelength λ_0 with an effectively narrow band-pass filter.

The radiated energy measured is

$$\epsilon(\lambda) J(\lambda, T) = J(\lambda, T_b)$$

or

$$\epsilon(\lambda) = \frac{J(\lambda, T_b)}{J(\lambda, T)} \quad (3)$$

Substituting Equation (1) in Equation (3) we obtain:

$$\epsilon(\lambda) = \frac{\frac{c_1 \lambda^{-5}}{c_1 \lambda^{-5}} \left[e^{\frac{c_2}{\lambda T_b}} - 1 \right]^{-1}}{\frac{c_1 \lambda^{-5}}{c_1 \lambda^{-5}} \left[e^{\frac{c_2}{\lambda T}} - 1 \right]^{-1}} \quad (4)$$

Planck's equation may be replaced by Wien's law as a suitable good approximation. We have then:

$$\epsilon(\lambda) = \frac{\frac{c_2}{\lambda T}}{\frac{c_1 \lambda^{-5}}{c_1 \lambda^{-5}} e^{\frac{c_2}{\lambda T_b}}}$$

or

$$\epsilon(\lambda) = e^{-\frac{c_2}{\lambda} \left(\frac{1}{T} - \frac{1}{T_b} \right)}$$

and finally

$$\frac{1}{T} - \frac{1}{T_b} = \frac{\lambda}{c_2} \ln \epsilon(\lambda) \quad (5)$$

which is the well known expression relating the emissivity to true and brightness temperatures of a real radiator. This expression was used in this analysis to compute the rare earth oxide specimen emittance, at $\lambda = 0.66 \mu\text{m}$, from measurements of true and brightness temperatures.

1. Thermocouple Method

As previously mentioned, the first method for obtaining emittance data at $\lambda = 0.66 \mu\text{m}$ was based on optical pyrometric measurement of surface brightness temperature, and on the use of a thermocouple implanted into the specimen for its true temperature evaluation. Specimens of 1" in diameter were formed around platinum/platinum-10% rhodium thermocouple junctions by dry pressing rare earth oxide powder in a cylindrical die with a fitted plunger. The plunger was provided with two parallel grooves along its length. These two grooves allowed the 0.25 mm diameter thermocouple leads to extend out of the die when the plunger was inserted. The location of the thermocouple junction inside the specimen is shown in Fig. 4.

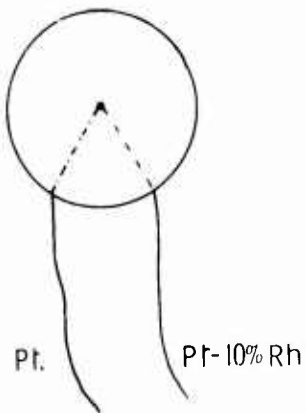


Fig. 4 - Location of the Thermocouple Junction Inside the Specimen

Figure 5 shows two of these specimens.

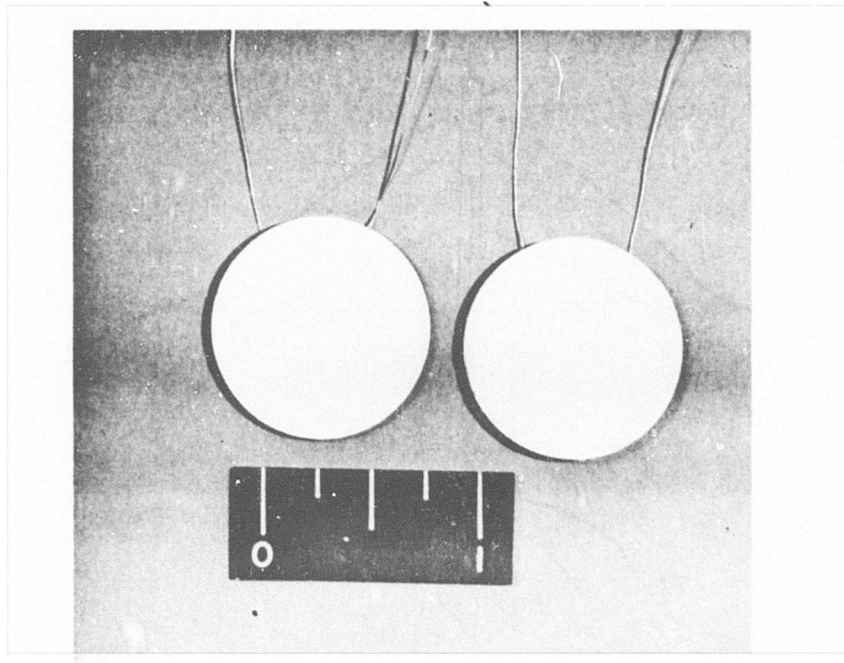


Fig. 5 - Er_2O_3 and Yb_2O_3 Specimens with Thermocouple Implanted

The specimen thickness was approximately 1-1.2 mm and, due to the low thermal conductivity of the samples, the use of only one oxygen-propane flame, impinging and heating the pellet from one side, proved to be inadequate for this test. Brightness temperature differences from 40° C up to 160° C, between the two specimens surfaces, were observed. The

ΔT 's are connected with the sample thickness, the thermal conductivity of the rare earth oxide material, and with the working temperature level. Therefore, the related transverse temperature gradient inside the pellet, where the thermocouple junction is located, completely masked any possible correlation between thermocouple output and true sample temperature. To overcome this problem, two oxygen-propane flames have been utilized to heat these specimens from both sides. Figure 6 is a drawing of the two-torch apparatus used for this series of measurements.

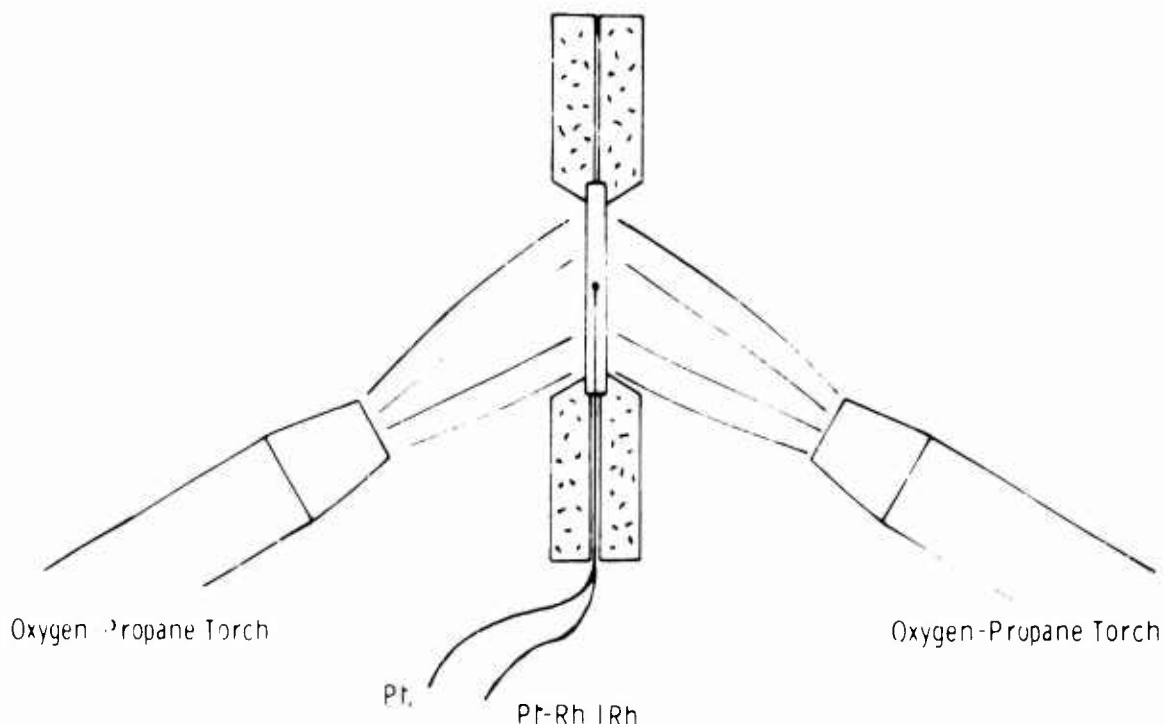


Fig. 6 - Two-Torch Apparatus used for Maintaining the Same Brightness Temperature on Both Sides of the Specimen

The two flames were adjusted in order to uniformly heat, on each side, a surface sample area of about 15 mm in diameter centered around the platinum/platinum-10% rhodium junction position. The thermocouple output was recorded only under conditions of equal brightness temperature on both surfaces. In this condition, due to the relevant ratio of uniformly heated surface area to sample thickness, a uniform temperature distribution from one side to the other in the central part of the pellet could be assumed. Therefore, the thermocouple output was taken as indicative of the true temperature of the specimen. The thermocouple leads were extended, with compensating lead wires, to a reference junction at 0° C, and the output recorded using a strip chart recorder.

The two implicit sources of error which can effect this determination of the true sample temperature are: (1) A change in the thermocouple junction performance due to the chemical interaction between the thermocouple junction and the sample materials at the high test temperatures encountered, and (2) A thermocouple output reduction due to the electrical conductivity of the specimen. To obtain an indication of a possible effect of chemical reactivity, some of the thermocouples used were carefully calibrated in a Leeds & Northrup furnace prior to their being assembled into the specimens. They were then utilized in emittance tests at temperatures ranging between 1450° K and 1870° K. Post experiment check of the thermocouple calibration, after their recovery from the samples, showed

agreement with the pretest calibration within 1 degree, attesting that no permanent changes in the junction performance of the thermocouple were experienced.

To obtain an indication of the effect of sample conductivity on the thermocouple output, some Er_2O_3 pellets were fabricated with two isolated platinum wire electrodes, 0.5 mm in diameter. The two electrodes were positioned, parallel and 2 mm apart, in the middle plane of the pellet, as shown in Fig. 7.

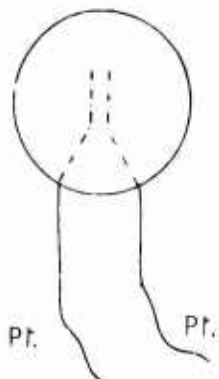


Fig. 7 - Location of the Two Parallel Platinum Electrodes Inside the Specimen

These specimens were heated, by oxygen-propane flame, to brightness temperatures of up to 2000° K. Increasing dc voltages, from 0.5 up to 92 volts, were applied to the platinum electrodes, and current-voltage characteristics obtained (see Appendix A).

From the values measured, electrical resistivities in the order of 10^2 ohm-meters were calculated at sample temperatures ranging between 1650° K and 2000° K. This range exceeds the maximum working temperature pyrometrically measured in the central area of the specimens where the thermocouple junction was located. Therefore, for the circumferential area of the samples, where the brightness temperatures detected are a few hundred degrees centigrade lower, and where a possible shunting of the thermocouple output can be taken in consideration, electrical resistivities of the order of 10^3 - 10^4 ohm-meters could be estimated. These resistivity values, as compared with the 10^{-6} ohm-meters platinum electrical resistivity, show that possible reduction of the thermocouple output could not be detected by the instrumentation used and, therefore, was assumed negligible. The true temperature obtained was applied in Equation (5) to calculate values of ϵ , at $\lambda = 0.66 \mu\text{m}$, for the sample specimens.

Since the direct emission of the oxy-propane flame at the pyrometric wavelength ($0.66 \mu\text{m}$) was found to be less than 10^{-3} of the

corresponding emission of the solid sample, errors in brightness temperature due to this effect were found not to exceed 1-2° C. Therefore, no substantial corrections to the observed values of T_b were required for use in Equation (5).

2. Cavity Method

The second method used to obtain emittance values at $\lambda = 0.66 \mu\text{m}$ was based on two pyrometric measurements obtained, respectively, from a flat surface element of the sample and from a small cavity, drilled into the sample, which behaves like a black body emitter. Therefore, the energy radiating from the cavity is indicative of the true temperature of the specimen. Figure 8 shows the section of two specimens, Yb_2O_3 and Er_2O_3 , respectively, in which cylindrically shaped cavities were formed.

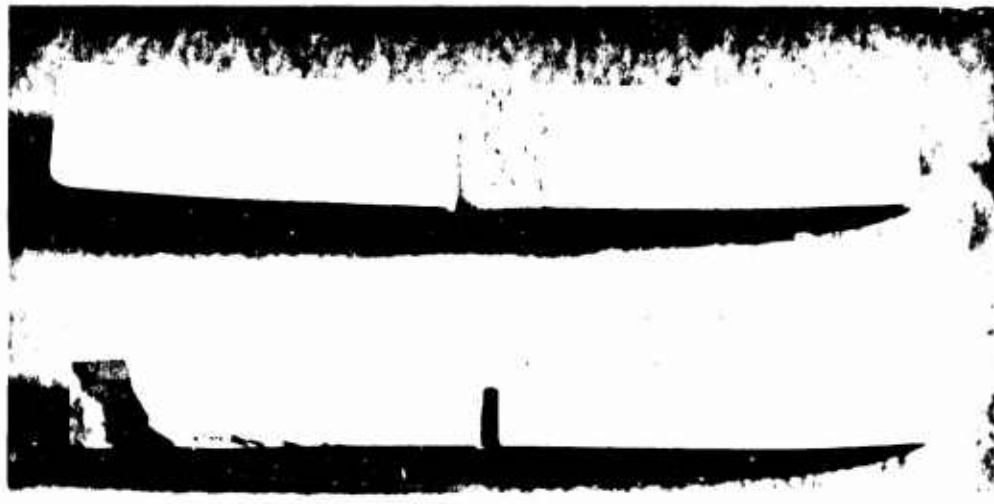


Fig. 8 - Section of Yb_2O_3 and Er_2O_3 Specimens Showing the Location of Cylindrical Cavities

In this series of measurements the sample thickness ranged from 2.2 to 4.3 mm and the cavity diameter ($2R$) varied from 0.57 to 0.78 mm. Cavity depths (d) were from 1.5 to 2.6 mm (Fig. 9).

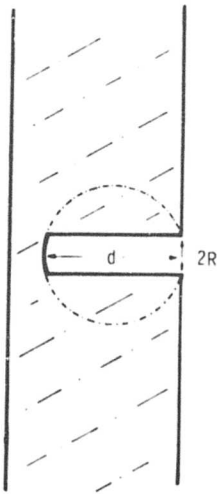


Fig. 9 - Cross Section of the Cylindrical Cavities Formed into the Specimens Used

These samples were also heated from both sides, and the pyrometric measurements were taken under conditions of exactly equal brightness temperature.

It was found that with increasing d/R up to values of 6, improvements in the emissivity values were experienced, but for d/R values above 6 no further improvement in the cavity emissivity was observed. Therefore, the sample true temperature taken in this evaluation was the one measured by sampling the radiation from cavities with d/R values between 6 and 7. For this geometry, the cavity behaves like an artificial black body with⁸ an emissivity approaching unity and expressed by the following relation:

$$\epsilon = (1 - \rho) \frac{\Omega}{\pi} \quad (6)$$

where ρ is the reflectivity of the material constituting the cavity, and

Ω is the solid angle under which radiation is emitted. Taking into account that $1 - \rho$ is the emissivity, ϵ_m , of the material constituting the cavity, and utilizing geometrical considerations connected to any possible cavity shape, Equation (6) can be rewritten as follows:

$$\epsilon = \frac{\epsilon_m}{\epsilon_m \left[1 - \frac{s}{S} \right] + \frac{s}{S}} \left[1 - K \right] \quad (7)$$

where s is the cavity aperture section, S is the cavity total surface and K is a number, positive or negative, but always close to one, expressed by the following relation:

$$K = \left(1 - \epsilon_m \right) \left[\frac{s}{S} - \frac{s}{S_0} \right] \quad (8)$$

S_0 being the surface of the sphere having the diameter equal to the cavity depth (See Figure 9). Using Equations (7) and (8), the emissivity, at $\lambda = 0.66 \mu\text{m}$, of the cavities for specimens of different rare earth oxide composition was evaluated. The ϵ_m value assumed for the four materials tested was the emittance value previously obtained, at the pyrometric wavelength, using the thermocouple method. The values of cavity emissivity obtained in this way were found to vary between 0.97 - 0.98, for the Er_2O_3 , and ranged down to 0.90 in the case of the Yb_2O_3 which displayed the lowest value, at $\lambda = 0.66 \mu\text{m}$, of the materials tested. This deviation from unity imposed a correction on the pyrometric measurements of the cavity temperature. Such a correction has been evaluated and found in the order of $4-5^\circ\text{C}$ for the Er_2O_3 and $13-14^\circ\text{C}$ for the Yb_2O_3 . The corrected true temperatures of the samples, together with their brightness temperatures, allowed the use of Equation (5) to calculate the emittance at $\lambda = 0.66 \mu\text{m}$. The values obtained show good agreement with those previously evaluated by the thermocouple method. They are plotted, as a function of sample true temperature, in Fig. 10.

3. Spectral Emittance

The emittance of a real body has been previously defined as the ratio of real body radiation to black body radiation at the same true temperature. A knowledge of the emittance value at $\lambda = 0.66 \mu\text{m}$ allows, by the use of an optical pyrometer, the setting of a rare earth oxide specimen and of a standard black body cavity to the same true temperature. Under these conditions, if the two emitting sources are seen by the entrance slit of a spectrophotometer with the same solid angle and path length, and if the monochromator spectral resolution corresponds to the band width of the pyrometer filter, then the ratio of the radiating energies, spectrometrically sampled from the rare earth oxide specimen and the black body cavity, will correspond to the emittance value previously determined, at $\lambda = 0.66 \mu\text{m}$, for the specimen material. This correlation procedure has been applied in this study to obtain the experimental determination of rare earth oxide spectral emittance.

Direct comparison of the sample and black body reference spectra at the entrance slit of a prism monochromator was accomplished by the time resolution of the combined beams using a 2 mirror beam-splitter chopper. A schematic design of the experimental layout is shown in Fig. 11, and the actual instrumentation used is illustrated in Fig. 12. The rare earth oxide specimens were mounted in a refractory material holder located, on

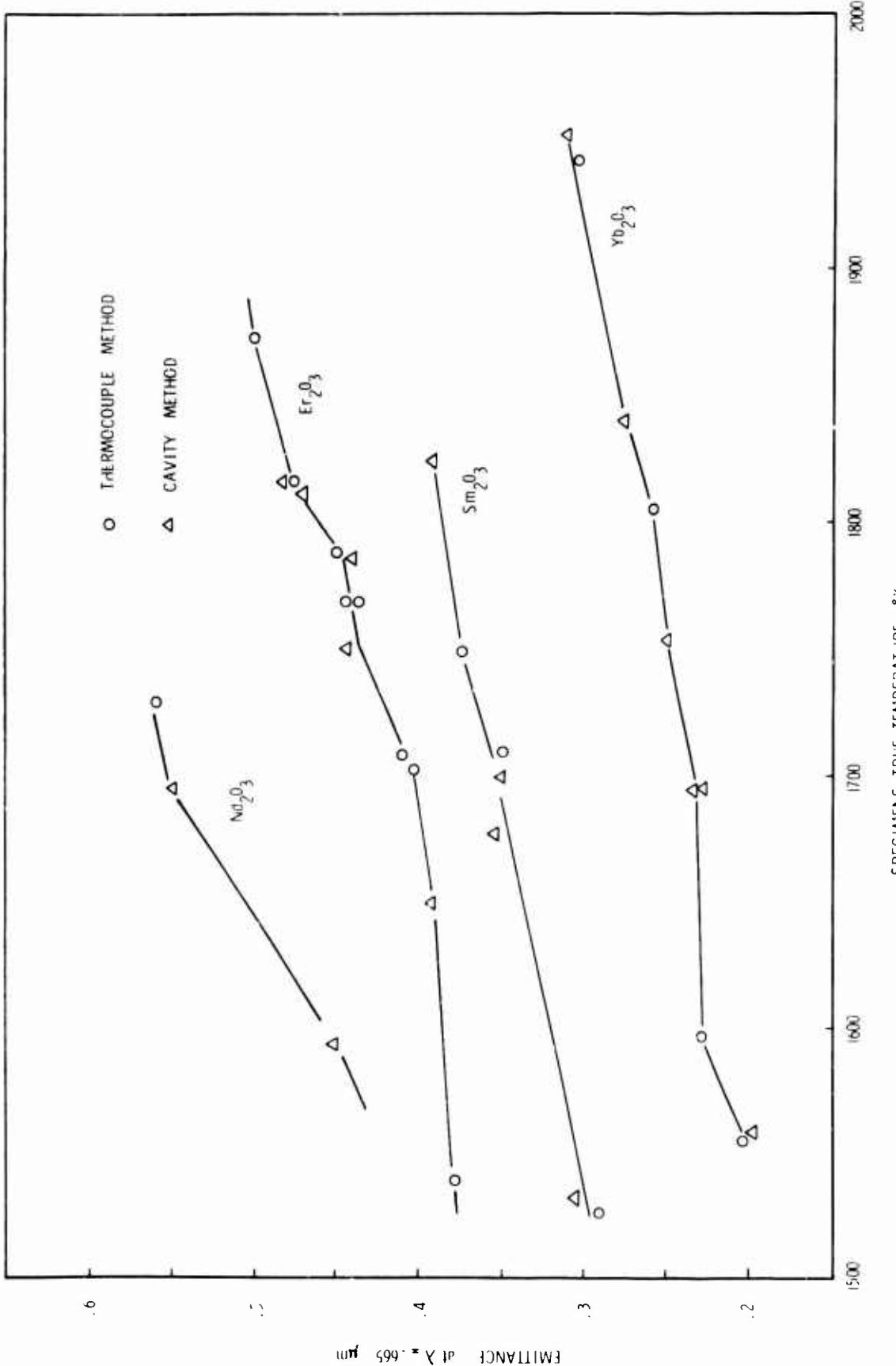


Fig. 10 - Emissance of Nd_2O_3 , Er_2O_3 , Sm_2O_3 and Yb_2O_3 in a Temperature Range Between 1500 and 2000° K

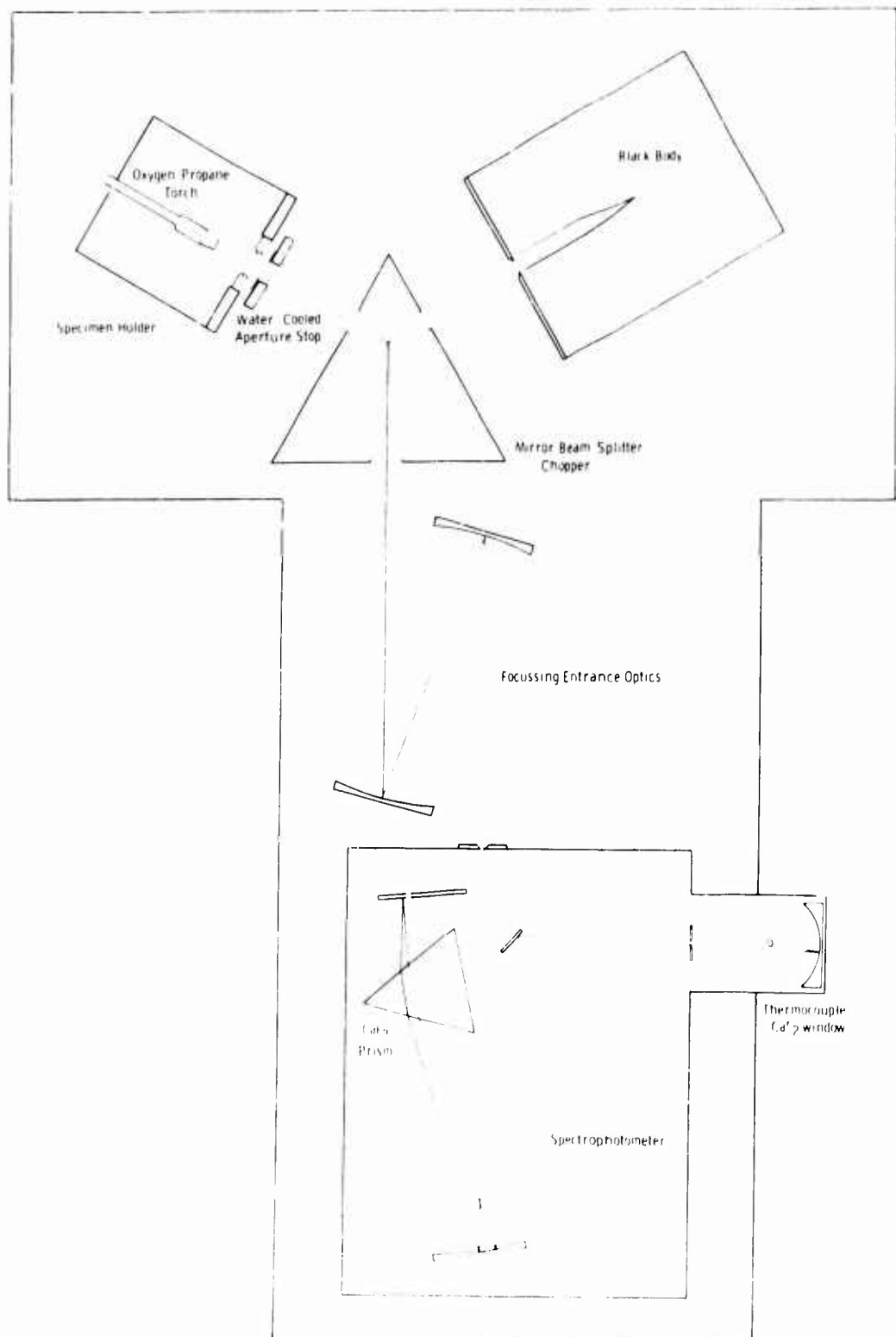
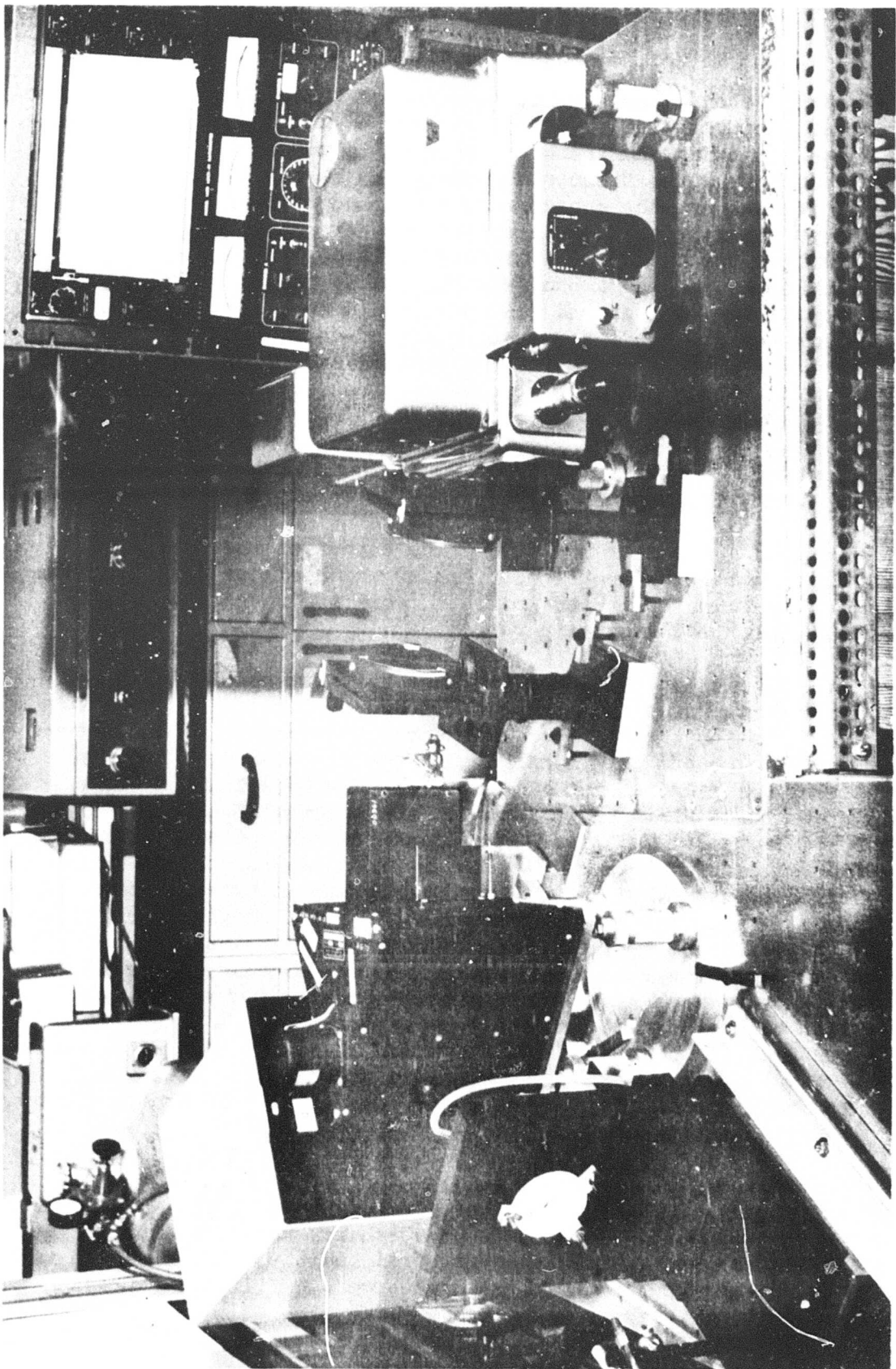


Fig. 11 - Schematic of the Instrumentation Assembly Utilized for the Emittance Spectra

Fig. 12 - Instrumentation Assembly



an adjustable interchangeable base, in front of the left entrance of the beam-splitter chopper. The sample discs were heated by only one oxygen-propane flame impinging and transferring heat to the sample on the back side. Radiation from the front side enters the beam-splitter chopper and then is focussed on the monochromator entrance slit. A water-cooled aperture stop, experimentally similar to the one constituting the exit of the black body cavity (6 mm in diameter), is positioned in front of the sample holder. The black body was located in front of the right entrance port of the chopper and also positioned on a similar mounting base. In this way the black body can be periodically interchanged with the sample to check the equality of the optical beam energy in the two paths. Both black body and sample aperture stops are positioned equidistantly from the monochromator entrance slit, which views the two emitting sources under the same solid angle. The monochromator used was from a Perkin Elmer Model 13U Spectrophotometer, equipped with a CaF_2 prism and with a CaF_2 window thermocouple detector. Two spherical mirrors, arranged to minimize off-axis aberrations, were used to bring the combined source beams to a focus at the entrance slit. The output of the thermocouple is amplified by a commercial lock-in-ratiometer which allows the simultaneous recording of the emission spectra of both radiating sources and their direct ratio over a 100:1 dynamic range.

An emittance spectral run was made by first setting both radiating sources to the same true temperature and then checking the output of the ratiometer for the value of emittance at $\lambda = 0.66 \mu\text{m}$ known from the previously described determinations. Spectral scanning was then conducted over the range 0.45 to 5.0 μm . For the selection of the monochromator resolution appropriate to match the spectral band width of the pyrometer filter, a careful evaluation of the filter characteristics had to be made. In case of materials, such as Er_2O_3 , which exhibit emission peaks centered around $\lambda = 0.66 \mu\text{m}$, the dissimilarity between spectrometer band-pass and pyrometer filter characteristics could result in critical errors in the emittance spectra recording. It is apparent that the procedures described depend on a correlation between photometric (luminance) and physical (radiance) systems of radiation measurement. The selection of the correct "effective wavelength" (λ_e) is of fundamental importance in relating the two systems of measurement, and becomes critical for materials whose spectra are not flat, radically deviating from a Plankian distribution, in the immediate vicinity of the pyrometer wavelength.

The effective wavelength of a monochromatic filter for a definite temperature interval is defined as the wavelength for which the relative brightness, as calculated from Wien's equation for this temperature interval, is the same as the ratio of the integral luminosities for these two temperatures, as measured through the monochromatic filter. Expressed in

the form of an equation, the following is the definition of the effective wavelength:

$$\frac{\int_0^{\infty} J(\lambda, T_1) t_r K_{\lambda} d\lambda}{\int_0^{\infty} J(\lambda, T_2) t_r K_{\lambda} d\lambda} = \left[\frac{J(\lambda, T_1)}{J(\lambda, T_2)} \right]_{\lambda_e} \quad (9)$$

where $J(\lambda, T)$ is the spectral distribution of the black body (Wien's equation); t_r is the spectral transmission of the monochromatic filter; K_{λ} is the relative luminosity factor of the eye, and λ_e is the effective wavelength. Thus, in practice, the effective wavelength is the weighted central value of the resulting band-pass characteristic obtained by applying the combined filter-eye characteristic to a particular radiant energy distribution. The effective wavelength presents a continuous shift towards the short wavelengths as the temperature increases, due to the related change in the radiant energy distribution.

Prior to recording the emittance spectra of Er_2O_3 , which shows an emission peak ranging from $0.64 \mu\text{m}$ up to $0.665 \mu\text{m}$, it was necessary to accurately evaluate the monochromator resolution at $\lambda = 0.66 \mu\text{m}$, and properly set the spectrometer drum, to correlate, at any working temperature, the corresponding effective wavelength of the pyrometer filter. Yb_2O_3 and Sm_2O_3 show no emission irregularities in the region of the effective wavelength, minimizing the above mentioned problem.

The resulting effective wavelength values, in the range of temperatures experimented in this analysis, are reported in Appendix B, together with the spectral characteristics utilized for the evaluation of the pyrometric band-pass filter width.

The major source of error which could affect the spectral emittance recording is connected with the accuracy of the starting emittance value at the pyrometric working wavelength. The previously mentioned sources of error which can affect the emittance evaluation at $\lambda = 0.66 \mu\text{m}$ will cause, if not corrected, a lower estimation of the specimen true temperature in both thermocouple and cavity methods. This will cause, as a consequence, a lower setting of the temperature of the black body reference source and, therefore, a comparison with an incorrect black body spectral energy distribution. Fortunately, due to the shift toward the short wavelength of the black body radiant energy distribution with increasing temperature, the spectral energy variation, as a function of the temperature, is lower in the infrared than in the visible part of the spectrum. An error of 20°C in the evaluation of the true temperature of the specimen could cause a 5-6% higher value in the evaluation of the emittance at $\lambda = 0.66 \mu\text{m}$, but only 3% in the emittance value at $1.1 \mu\text{m}$ and less than 2% beyond $1.6 \mu\text{m}$ region.

The accuracy of the brightness temperature measurements is related to the reliability of the optical pyrometer used. The calibration of this instrument was constantly controlled against the black body calibration curve, and the entire set of temperatures utilized for this analysis can then be considered self consistent, therefore, not effecting the validity of the emittance spectra obtained.

Figures 13 thru 20 show the spectral emittance curves which are characteristic of the samples of the 4 rare earth oxides investigated. For reasons of clarity, the emittance curves shown are given for only a few temperatures. At intermediate temperatures, a linear interpolation can be employed.

The emittance at the strong, broad peak shown for Er_2O_3 at 1.54 μm (Fig. 13) rises rapidly, with temperature, to values around 0.55, but does not intensify significantly at higher excitation levels as other parts of the spectrum. This behavior agrees with and explains the results of a previous germanium cell - rare earth oxide system evaluation³ which showed, for the Er_2O_3 emission, a spectral utilization exhibiting a slightly negative slope with increasing total radiant power density.

The high average value of the spectral emittance of Sm_2O_3 (Figures 15 & 16) and Nd_2O_3 (Figures 17 & 18) explains the high levels of total radiant power density easily achieved with specimens of these two materials, as radiant emitters, in previous studies.³ Similarly, the impossibility of previously achieving radiant surface density levels higher than 18 watts/cm² with specimens of Yb_2O_3 is also understandable by observing (Figures 19 & 20) that at 0.95 μm , where Yb_2O_3 shows its strong peak, the spectral energy amount is relatively small and beyond 1 μm the emittance of this material is particularly low.

Transmission spectra^{10,11} of the rare earth oxides dissolved in glasses show atomic absorption bands characteristic of the trivalent anions. These correspond to the emittance spectra found in the present study with the exception of a 1.09 μm band which is observed in Nd_2O_3 emission but missing in absorption spectra. As expected, these emission spectra show considerable broadening due to the thermal mechanism of sample excitation.

Sample Absorptance and Reflectance

From the geometry of the specimen and the refractory properties of the sample holder, which is also heated by the oxygen-propane flame in the vicinity of the pellet circumference, the transverse energy losses occurring in the mounting arrangement were minimized. Consequently, the central portion of the specimen, in a zone of 3 mm radius from the optical axis corresponding to the sampling area when viewed thru the water cooled aperture stop, could be assumed to be in a condition of thermal equilibrium with its immediate surrounding. Thus, in the sampling area, we may consider that energy is being emitted at the same rate as it is being absorbed. The emissivity, reflectivity and

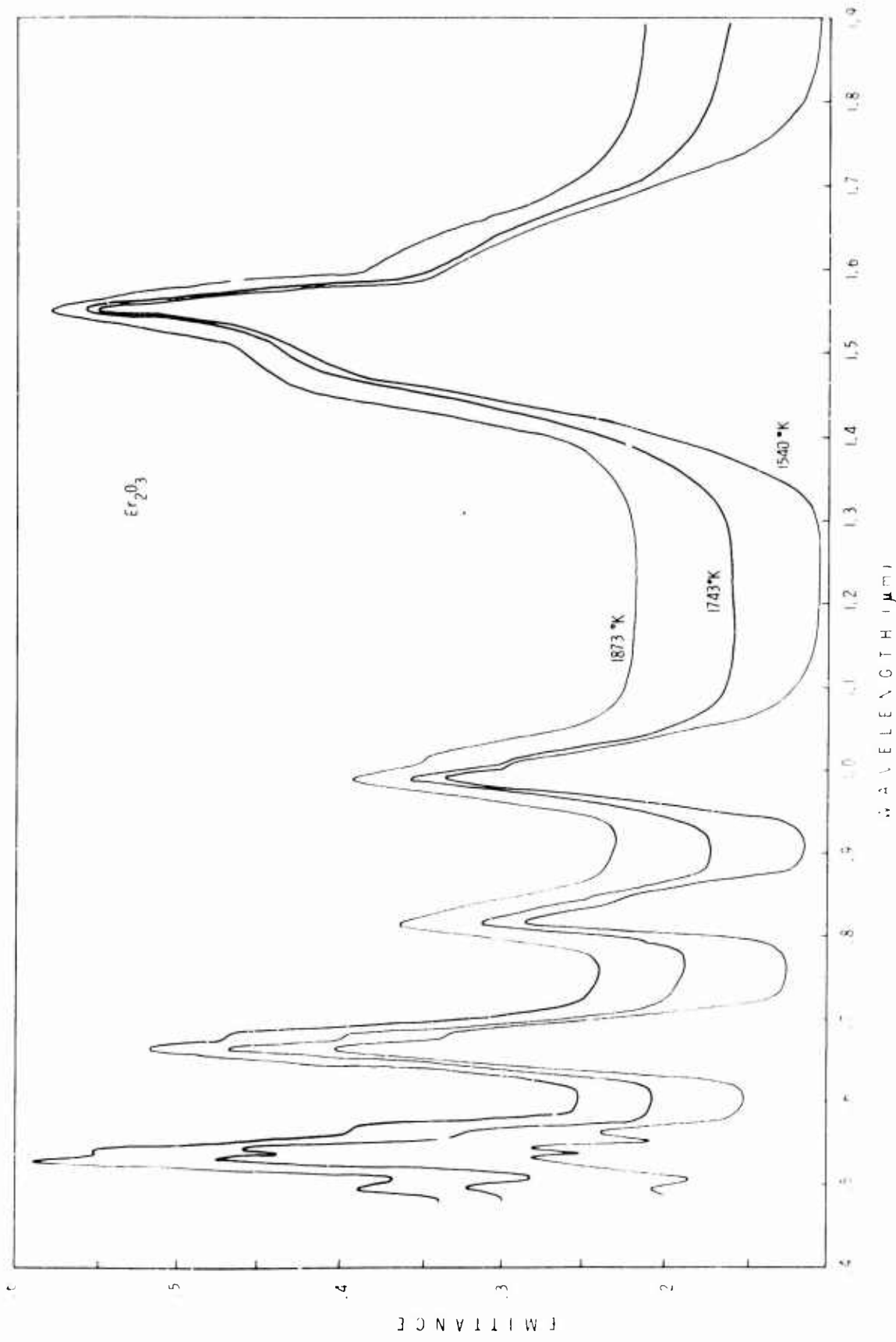


Fig. 13 - Spectral Emittance of Er_2O_3 in a Wavelength Range from .45 μm to 1.9 μm

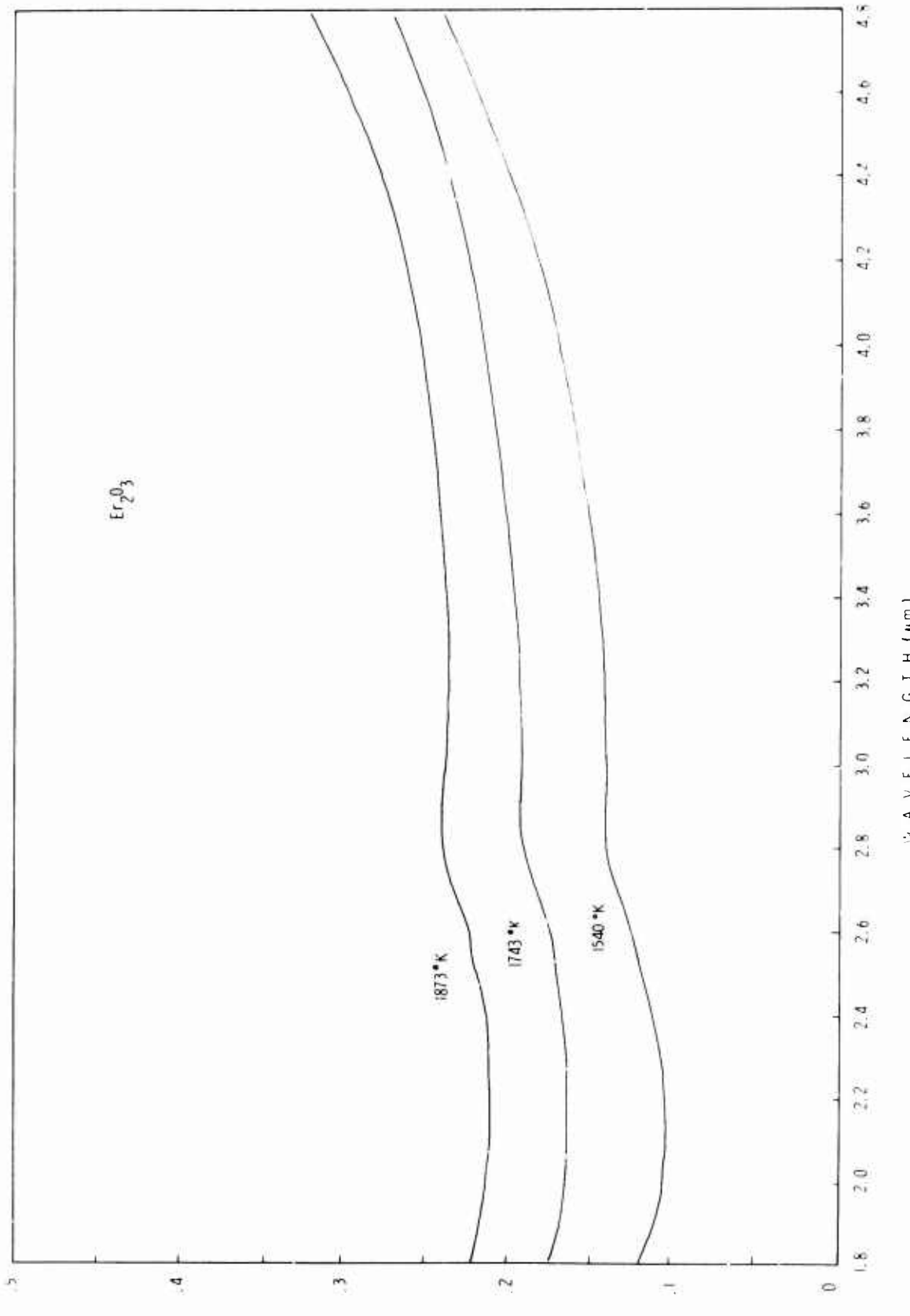


Fig. 14 - Spectral Emissance of Ba_2O_3 in a Wavelength Range from 1.8 μm to 4.8 μm

E M I T T A N C E

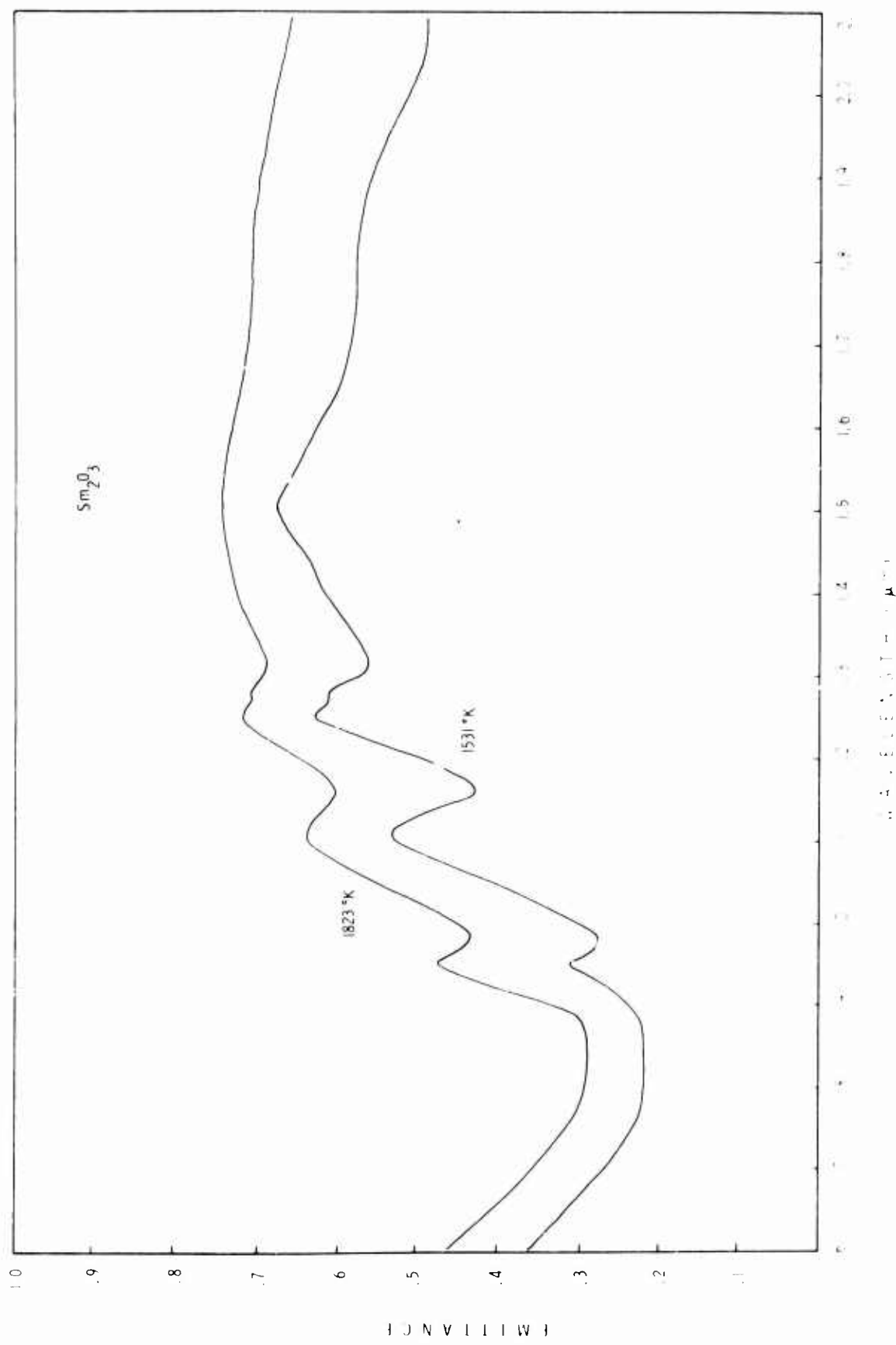


Fig. 15 - Spectral emittance of Sm_2O_3 in a wavelength range from 0.6 μm to 2.1 μm

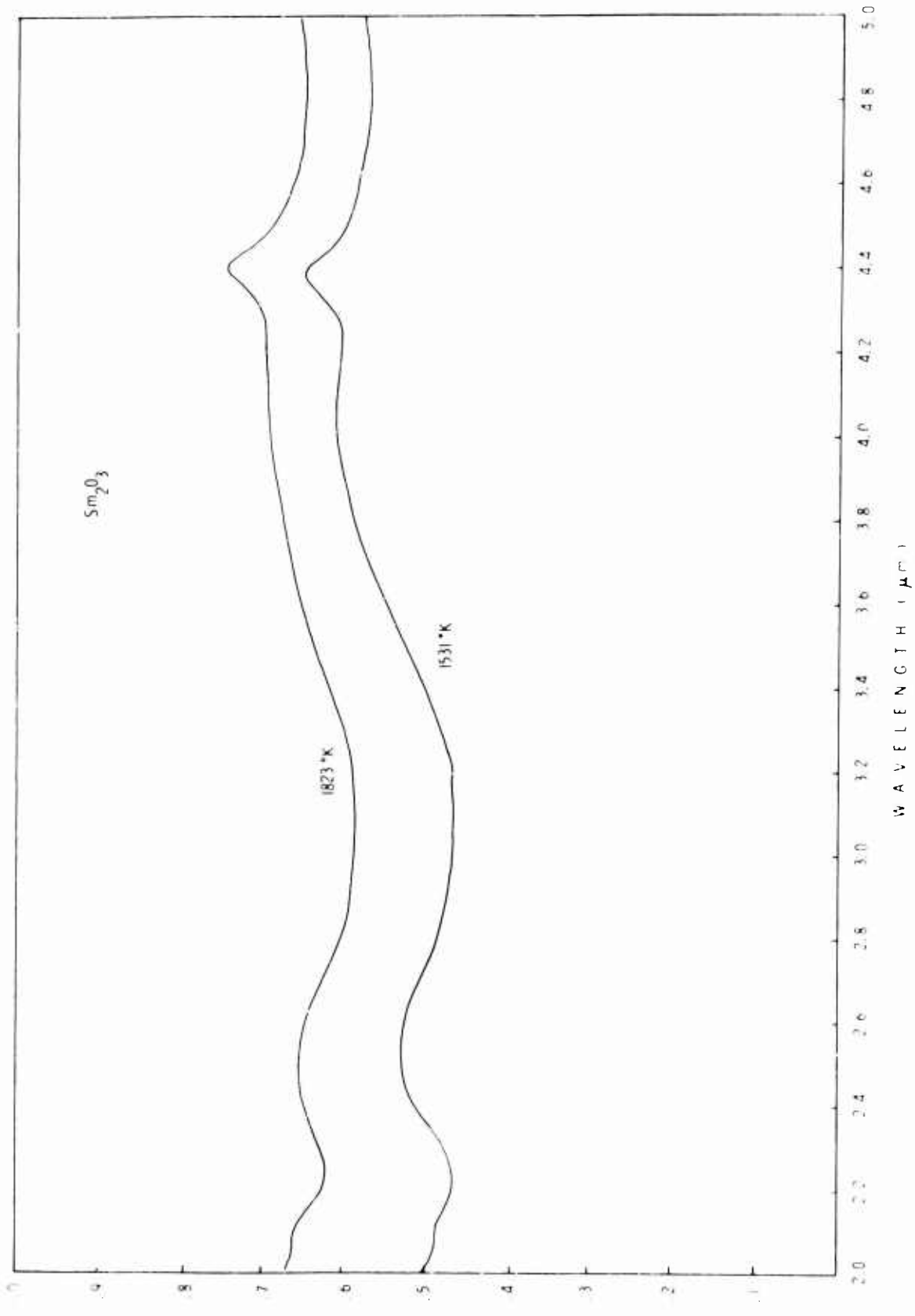


Fig. 16 - Spectral Emissance of $\text{S}_{\text{2}\text{O}_3}$ in a Wavelength Range from 2.0 μm to 5.0 μm

MITTANCE

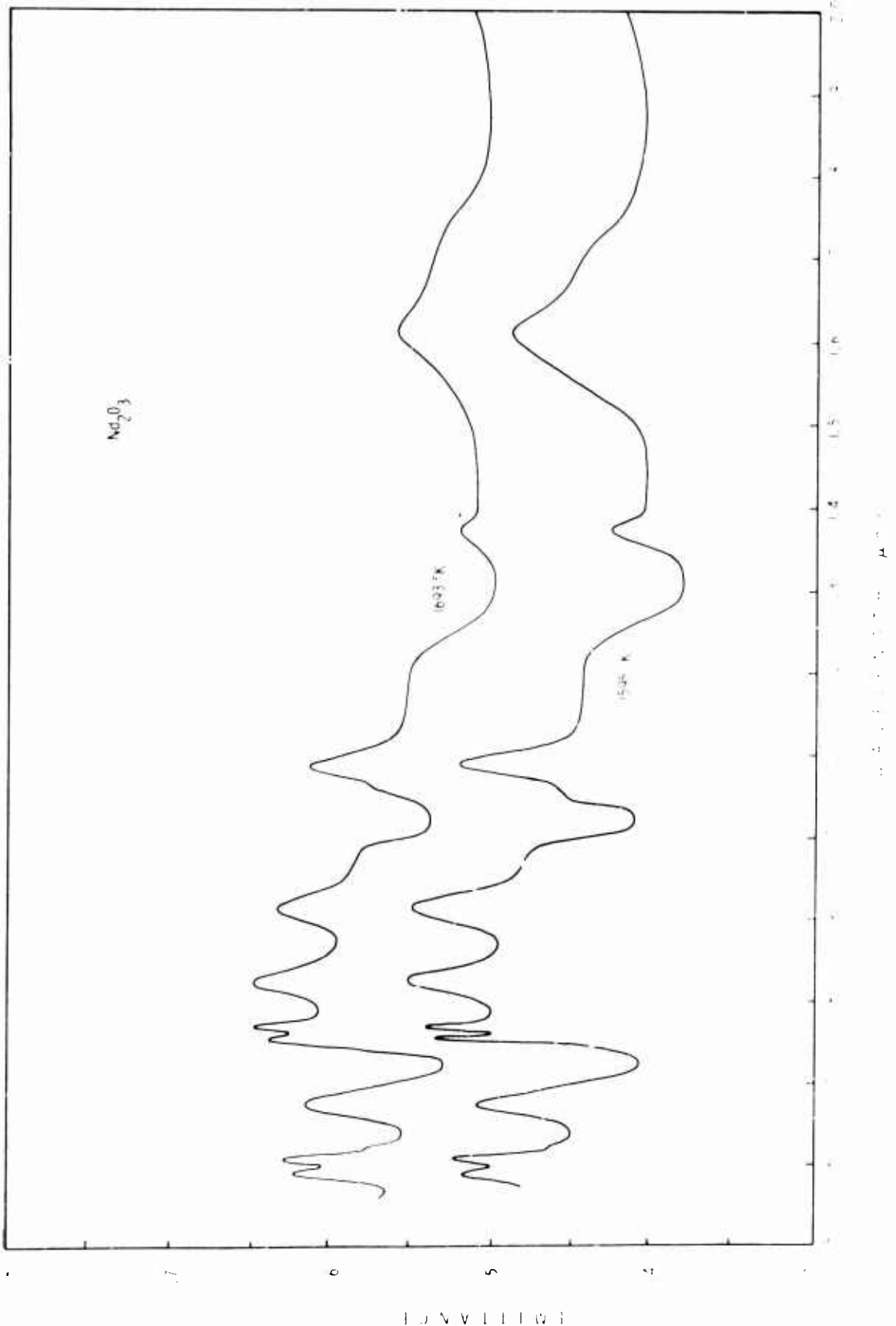


Fig. 1' - Spectral Emittance of Nd_2O_3 in a Wavelength Range from 0.55 μm to 2.0 μm

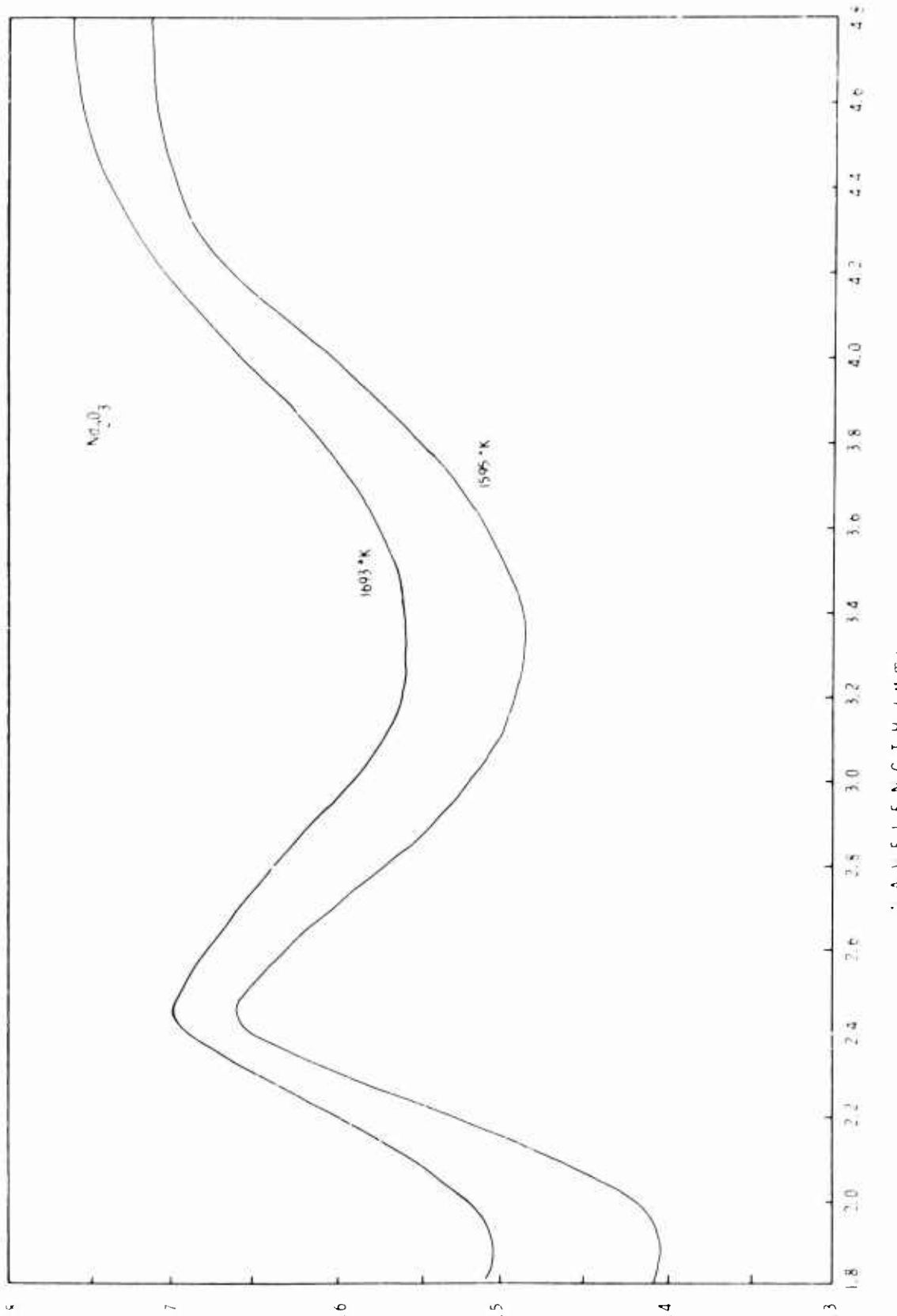


Fig. 18 - Spectral Emissance of Nd_2O_3 in a Wavelength Range from 1.8 μm to 4.8 μm

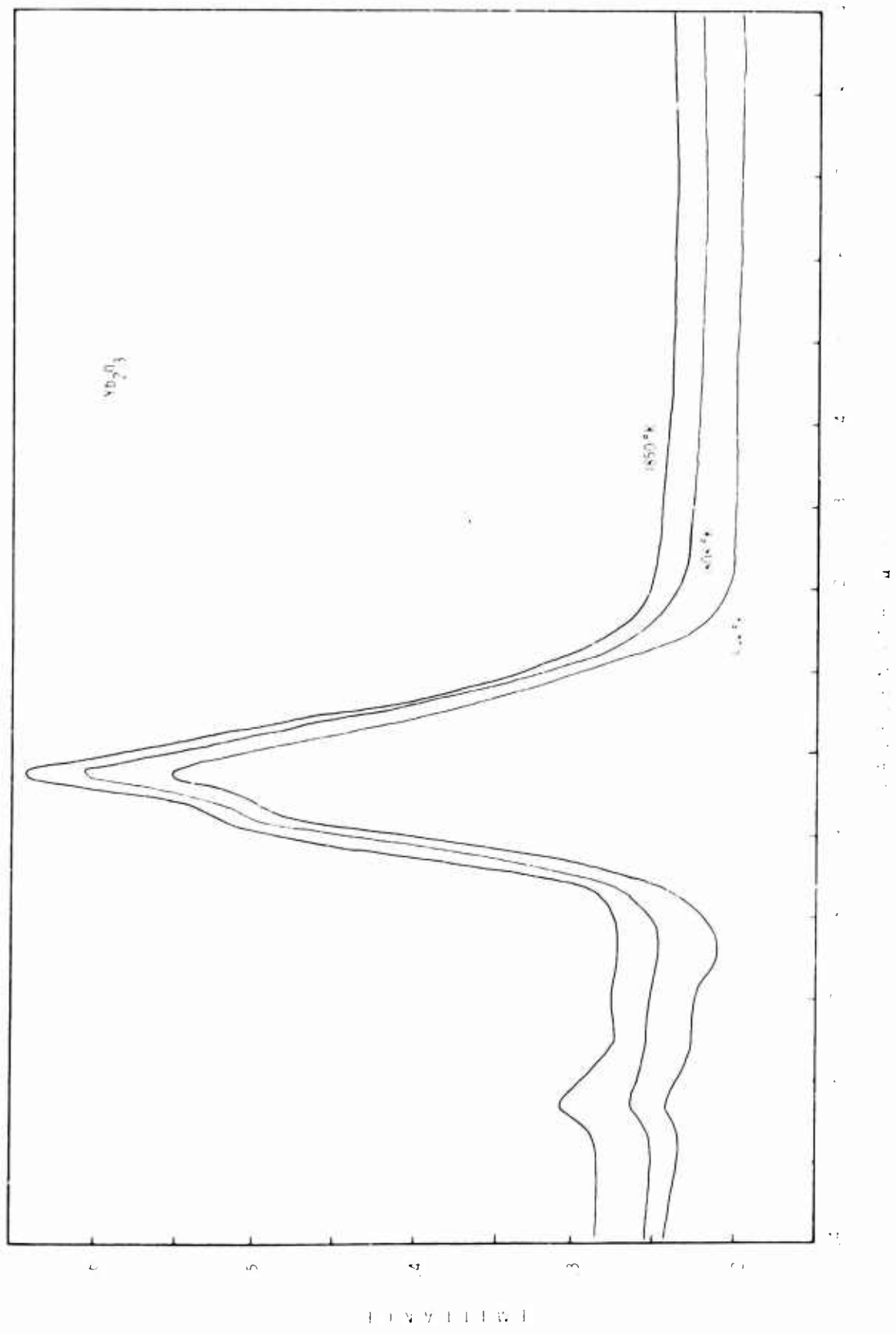


Fig. 19 - Spectral Emissance of Yb_2O_3 in a Wavelength Range from 0.4 μm to 1.9 μm

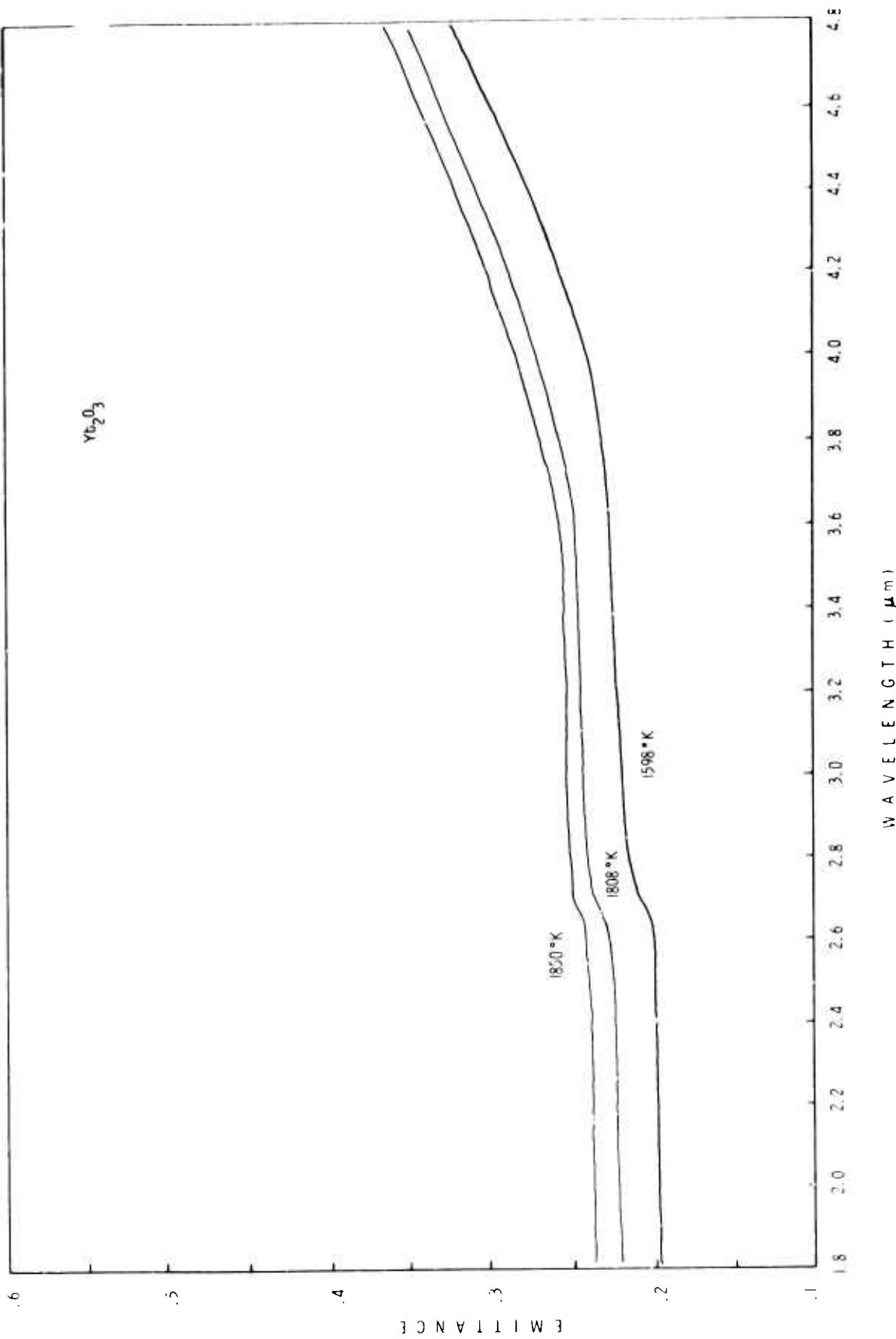


Fig. 20 - Spectral Emissance of Yb_2O_3 in a Wavelength Range from 1.8 μm to 4.8 μm

absorptivity properties of the specimen can then be related using Kirchoff's law. It states:

$$\epsilon = \alpha \quad (10)$$

$$\alpha + \rho + \tau = 1 \quad (11)$$

with

ϵ = emittance

α = absorptance

ρ = reflectance

τ = transmittance

From the results of the tests described above, we can assume the transmittance as negligible for radiant energy normal to the sample surface. With the assumption of sample opacity, the spectral emittance is equivalent to spectral absorptance and, from Equation (12),

$$\rho = 1 - \epsilon \quad (12)$$

spectral reflectance of the samples can be directly obtained.

CONCLUSIONS

Accurate determination of the spectral emittance of a solid sample can be made by direct comparison of its emission with that of a black body radiator provided both emitters are at the same true temperature. In this study, specimen true temperature was obtained by means of both the embedded thermocouple and the cavity methods and was related to the temperature determined by optical pyrometry. By evaluating the pyrometer effective wavelength and pyrometer filter band width, we found good correlation between pyrometric and photometric methods at a singular wavelength which permitted direct recording of spectral emittance using a scanning monochromator.

The absolute spectral emittances of the oxides of Erbium, Ytterbium, Samarium and Neodymium exhibited considerable spectral structure in the visible and near infrared which, in virtually all cases, showed direct correspondence with trivalent absorption spectra. Neither Nd_2O_3 nor Sm_2O_3 exhibit sufficient "spectral selectivity" to warrant further consideration as radiant sources for optimizing the thermophotovoltaic

energy conversion scheme. Nd_2O_3 , because of its high deliquescence, would also prove to be an impractical material to use in a radiant energy conversion power source. Er_2O_3 is well suited for spectral matching to germanium photovoltaic cells and has a relatively low emittance in the infrared beyond 1.7 μm . It is of interest to note that Er_2O_3 emittance in the visible and near infrared can be matched effectively to silicon photovoltaic cells if used with suitable filtration at 1.2 μm . Yb_2O_3 emittance can provide a useful match with silicon cells with good spectral selection provided by the low emittance beyond 1.2 μm . The spectral emittance characteristics obtained will be utilized for a complete analysis of the entire system, consisting of a rare earth oxide source emitter and germanium or silicon cell converter. For this analysis, reflectance data will be also needed. Experimental studies are in progress to characterize the spectral reflectance of these materials from the direct analysis of the radiation scattered from the sample surface.

ACKNOWLEDGMENT

The authors are indebted to their colleague, Dr. E. Kittl, for helpful discussions which have essentially contributed to the solution of problems dealt with in this work.

REFERENCES

1. E. Kittl, "Thermophotovoltaic Energy Conversion," Proc. 20th Annual Power Sources Conference, pp. 178-182, May 1966.
2. G. Guazzoni, E. Kittl and S. Shapiro, "Rare Earth Radiators for Thermophotovoltaic Energy Conversion," 1968 International Electron Devices Meeting, IEEE, October 1968.
3. G. Guazzoni, "Rare Earth Oxide Radiators for Thermophotovoltaic Energy Conversion," - Research and Development Technical Report ECOM-3116, April 1969.
4. W. R. McMahon and D. R. Wilder, "High Temperature Spectral Emissivity of Yttrium, Samarium, Gadolinium, Erbium and Lutetium Oxides," Report IS-578, January 1963, Ames Laboratory, Iowa State University of Science and Technology.
5. Allison Division, General Motors Corp., Final Report, "Radiant Energy Conversion(U)," 10 March 1967, Contract AT(30-1)-3587 (USAEC).
6. A. G. Worthing, "Temperature Radiation Emissivities and Emittances," Temperature, Its Measurement and Control in Science and Industry - American Institute of Physics (Reinhold Publishing Corp., New York, 1941) pp. 1164-1187.
7. G. D. Nutter, "General Considerations Influencing the Design of a High-Accuracy Pyrometer," Temperature, Its Measurement and Control in Science and Industry - American Institute of Physics (Reinhold Publishing Corp., New York, 1962).

8. A. Gouffe, "Corrections D'Ouverture Des Corps Noirs Artificiels Compte Tenu Des Diffusions Multiples Internes," *Revue D'Optique* 24, 1 (1945).
9. W. E. Forsythe, "Optical Pyrometry," *Temperature, Its Measurement and Control in Science and Industry - American Institute of Physics* (Reinhold Publishing Corp., New York, 1941) pp. 1115-1131.
10. Given W. Cleek (Inorganic Materials Division, National Bureau of Standards, Washington, D. C.) - Private Communication.
11. Richard F. Woodcock, "Multiple Doped Erbium Glasses," *Research and Development Technical Report ECOM-0313-1-2-3*, July 1969.

APPENDIX A

Evaluation of Sample Resistivity

Some of the current-voltage characteristics obtained during the experiment described in the paragraph on Thermocouple Method are reported in Figure 21. The samples used were fabricated with Er_2O_3 powder and had an apparent density around 4.8. The two implanted platinum wires were 0.5 mm in diameter and arranged to give a parallel section 8 mm long and 2 mm apart (See Figure 7). Voltages, increasing from 1.5 volts to 92 volts, were applied to the electrodes and the resulting current plotted, as shown in Figure 21. The linear relationship indicates the ohmic behavior of Er_2O_3 over the range of temperature and electric field studied. At 2000°K and 92 volts, a sharp increase in current was noted resulting from the formation of a liquid phase in the interelectrode zone. This effect was not investigated further to determine what caused melting to occur.

The approximate resistivity values obtained from these experimental data correspond to 200 ohm-meters at sample temperature of 1650°K , and 33 ohm-meters at sample temperature around 2000°K .

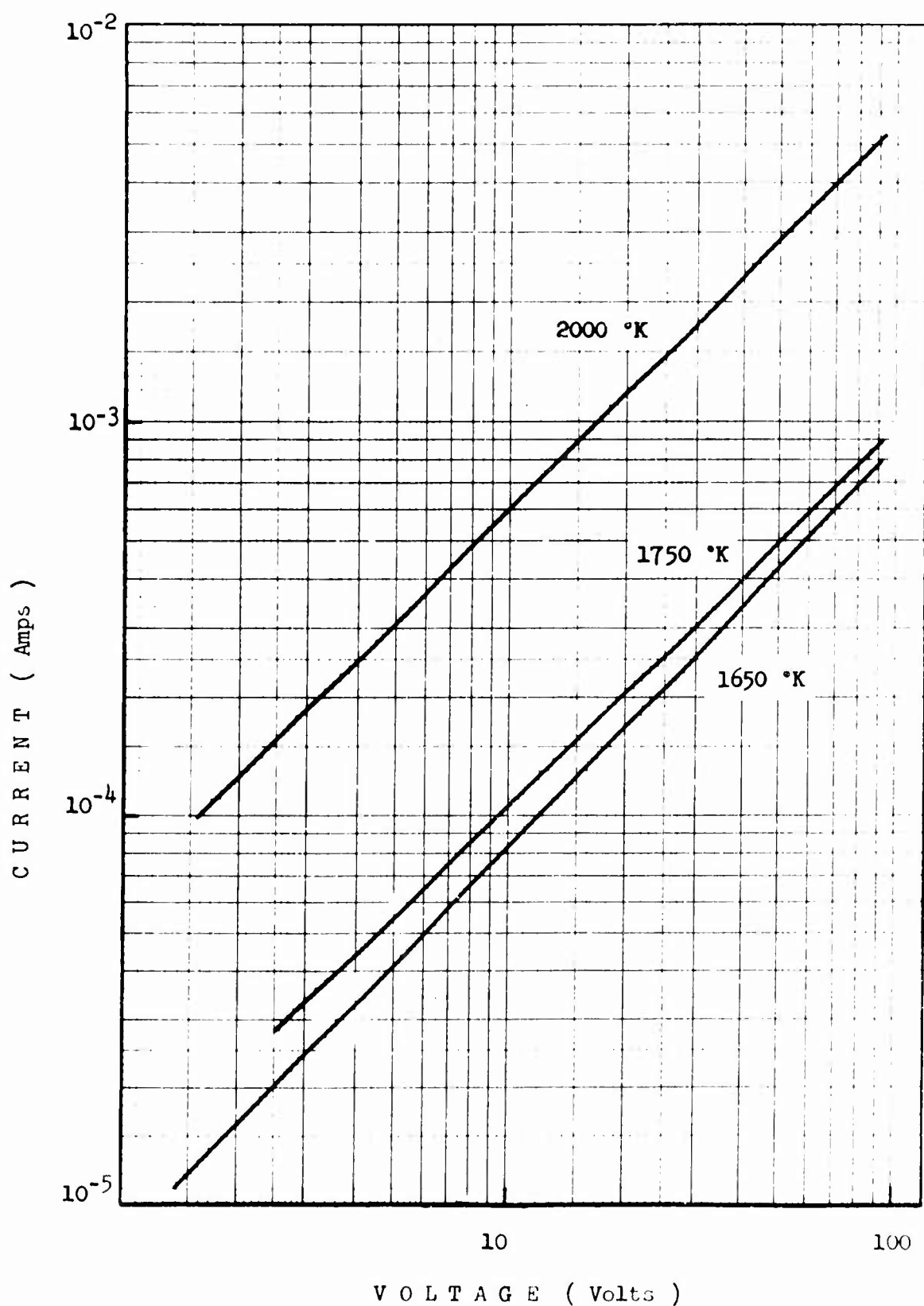


Fig. 21 - Er_2O_3 Electrical Resistance Characteristics

APPENDIX B

Determination of Pyrometer Effective Wavelength

In Figure 22 the relative eye luminosity factor and the optical transmittance of the Corning #2403 red glass filter, utilized for the computation of the pyrometric filter band-pass characteristic, are reported. The resulting band-pass characteristic, plotted in terms of relative transmittance, is given in Fig. 23. Figure 24 shows the corresponding effective wavelength for any temperature interval in the range 1300 - 3000 K.

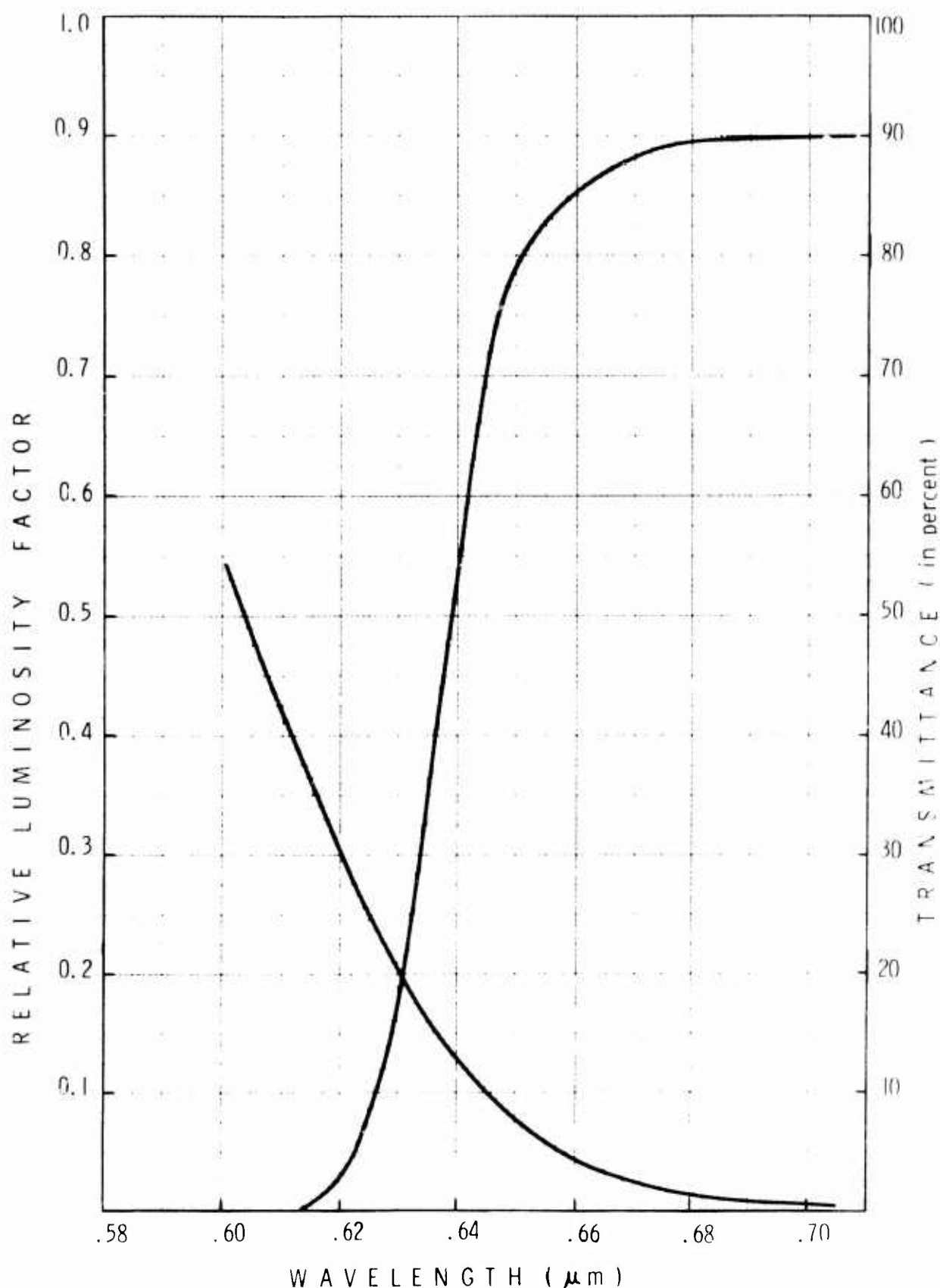


Fig. 22 - Relative Eye Luminosity Factor and Optical Transmittance of the Corning #2403 Red Glass Filter

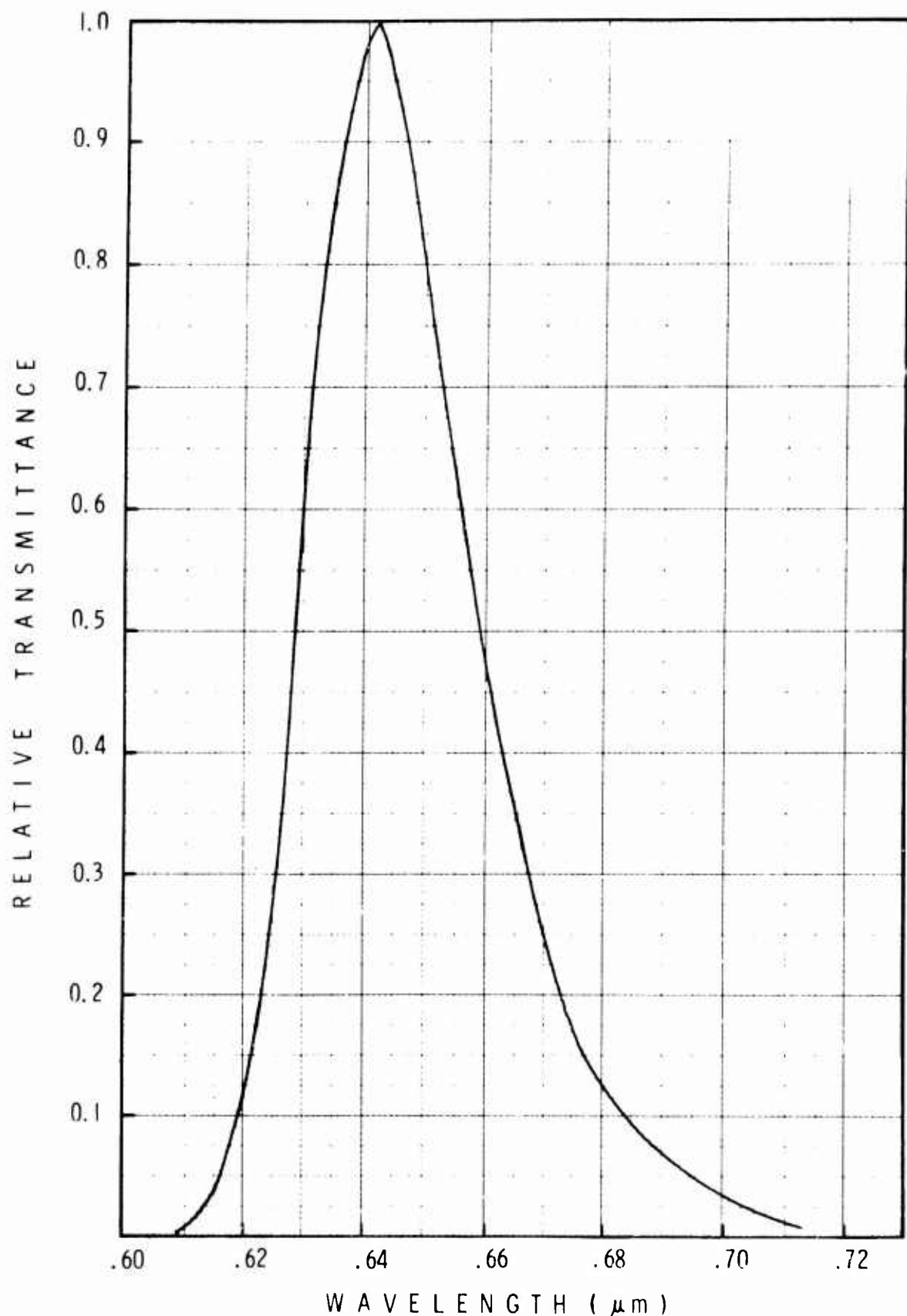


Fig. 23 - Pyrometer Filter Band-Pass Characteristic

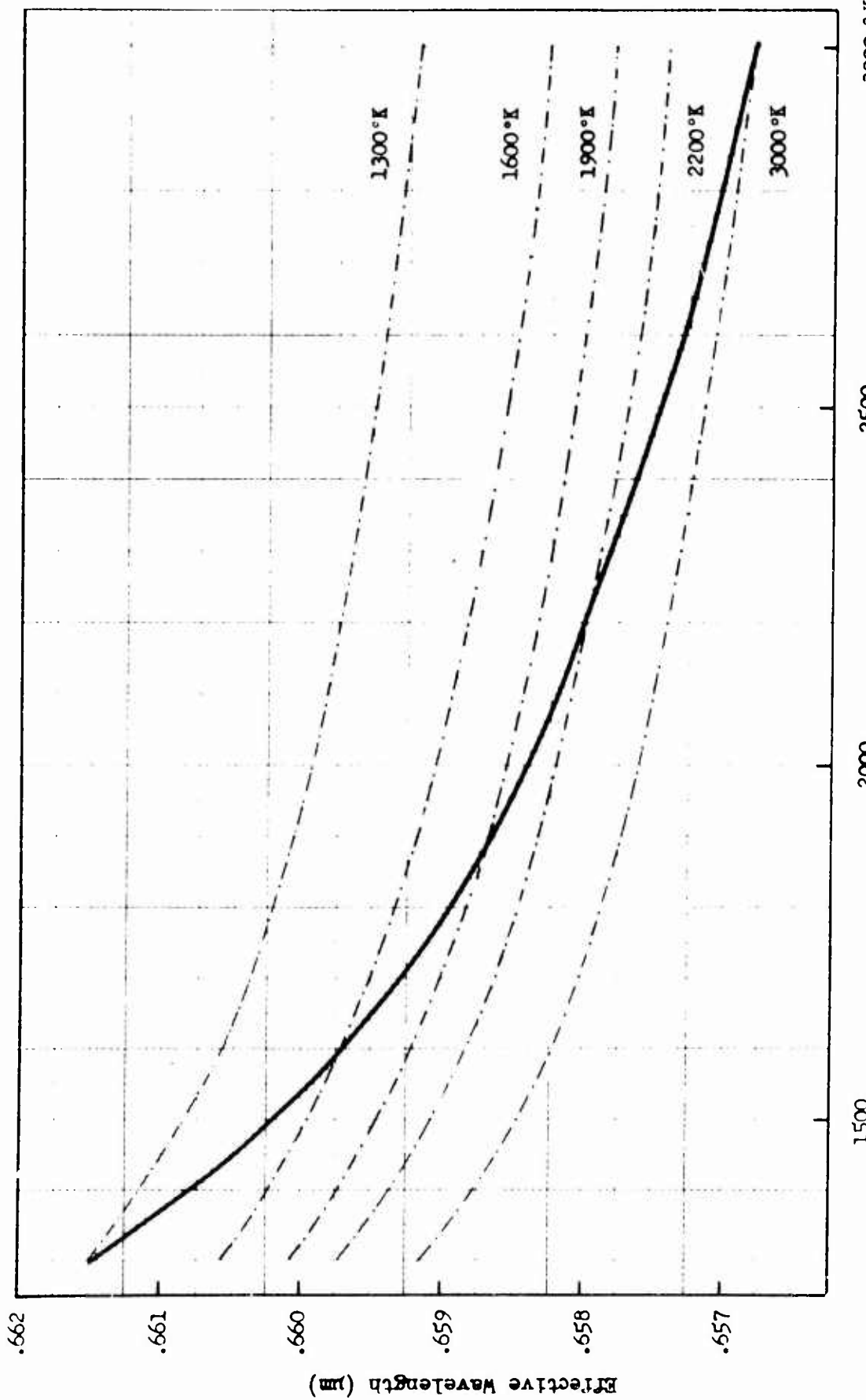


Fig. 24 - Effective Wavelength for any temperature Interval in the Range $1300 - 3000^{\circ}$ K.

Security Classification

DOCUMENT CONTROL DATA - R & D

(Security classification of title, body of abstract and indexing annotation must be entered when the overall report is classified)

1. ORIGINATING ACTIVITY (Corporate author) US Army Electronics Command Fort Monmouth, New Jersey 07703		2a. REPORT SECURITY CLASSIFICATION Unclassified
2b. GROUP		
3. REPORT TITLE SPECTRAL EMITTANCE OF NEODYMIUM, SAMARIUM, ERBIUM AND YTTERBIUM OXIDES AT HIGH TEMPERATURE		
4. DESCRIPTIVE NOTES (Type of report and inclusive dates) Technical Report		
5. AUTHOR(S) (First name, middle initial, last name) Guido E. Guazzoni and Stuart J. Shapiro		
6. REPORT DATE May 1970	7a. TOTAL NO. OF PAGES 37	7b. NO. OF REFS 11
8a. CONTRACT OR GRANT NO	9a. ORIGINATOR'S REPORT NUMBER(s)	
b. PROJECT NO. 1TO 61102 A 34 A	ECOM-3281	
c. Task -02	9b. OTHER REPORT NO(S) (Any other numbers that may be assigned this report)	
d. Subtask -31		
10. DISTRIBUTION STATEMENT This document has been approved for public release and sale; its distribution is unlimited.		
11. SUPPLEMENTARY NOTES	12. SPONSORING MILITARY ACTIVITY US Army Electronics Command Attn: AMSEL-KL-PE Fort Monmouth, New Jersey 07703	
13. ABSTRACT Spectral emittance of solid specimens of Er_2O_3 , Yb_2O_3 , Sm_2O_3 and Nd_2O_3 has been obtained by comparison of sample emission with the emission of a standard black body cavity maintained at the same sample true temperature. The spectral emittance has been characterized in a wavelength range of 0.4 - 5.0 micrometer and at sample temperatures from 1520°K up to 1870°K corresponding to surface radiation flux densities of $10 - 50 \text{ W/cm}^2$. This flux density range is of practical interest for thermophotovoltaic energy conversion applications. Preliminary observations of spectral transmittance and reflectance are also reported.		

DD FORM 1473 1 NOV 68

REPLACES DD FORM 1473, 1 JAN 64, WHICH IS
OBsolete FOR ARMY USE.

(1)

Security Classification

Security Classification

14 KEY WORDS	LINK A		LINK B		LINK C	
	ROLE	WT	ROLE	WT	ROLE	WT
Thermophotovoltaic Emissivity Emittance Transmittance Absorptance Reflectance Rare-Earth Oxides Selective Radiators						

(2)